HHS Public Access

Author manuscript

Cell. Author manuscript; available in PMC 2024 June 17.

Published in final edited form as:

Cell. 2023 May 11; 186(10): 2062–2077.e17. doi:10.1016/j.cell.2023.03.033.

Enveloped viruses pseudotyped with mammalian myogenic cell fusogens target skeletal muscle for gene delivery

Sajedah M. Hindi[1], **Michael J. Petrany**[1], **Elena Greenfeld**[2], **Leah C. Focke**[1], **Alyssa A.W. Cramer**[1], **Michael A. Whitt**[3], **Ramzi J. Khairallah**[4], **Christopher W. Ward**[5], **Jeffrey S. Chamberlain**[6], **Vikram Prasad**[1], **Benjamin Podbilewicz**[2], **Douglas P. Millay**[1,7,*]

[1]Division of Molecular Cardiovascular Biology, Cincinnati Children's Hospital Medical Center, Cincinnati, OH, USA.

[2]Department of Biology, Technion-Israel Institute of Technology, Haifa, Israel.

[3]Department of Microbiology, Immunology, and Biochemistry, University of Tennessee Health Science Center, Memphis, TN, USA.

[4]Myologica, LLC, New Market, MD, USA.

[5]Department of Orthopedics and Center for Biomedical Engineering and Technology (BioMET), University of Maryland School of Medicine, Baltimore, MD, USA.

[6]Departments of Neurology, Medicine and Biochemistry, Wellstone Muscular Dystrophy Specialized Research Center, University of Washington School of Medicine, Seattle, WA, USA.

[7]Department of Pediatrics, University of Cincinnati College of Medicine, Cincinnati, OH, USA.

Summary

Entry of enveloped viruses into cells is mediated by viral fusogenic proteins that drive membrane rearrangements needed for fusion between viral and target membranes. Skeletal muscle development also requires membrane fusion events between progenitor cells to form multinucleated myofibers. Myomaker and Myomerger are muscle-specific cell fusogens, but do not structurally or functionally resemble classical viral fusogens. We asked if the muscle fusogens could functionally substitute for viral fusogens, despite their structural distinctiveness, and fuse viruses to cells. We report that engineering of Myomaker and Myomerger on the membrane of enveloped viruses leads to specific transduction of skeletal muscle. We also demonstrate that locally and systemically injected virions pseudotyped with the muscle fusogens can deliver μDystrophin to skeletal muscle of a mouse model of Duchenne muscular dystrophy and alleviate pathology. Through harnessing the intrinsic properties of myogenic membranes, we establish a platform for delivery of therapeutic material to skeletal muscle.

*Lead contact: douglas.millay@cchmc.org.

Author contributions

S.M.H., B.P., and D.P.M. conceived the project. S.M.H., M.J.P., E.G., L.F., A.A.W.C., R.J.K., C.W., and V.P. conducted experiments and analyzed the data. M.A.W., J.S.C., B.P., and D.P.M. supervised the project. S.M.H. and D.P.M. wrote the manuscript with input from all authors.

Declaration of interests

The authors declare competing financial interests: S.M.H. and D.P.M. have filed patent applications on this work through Cincinnati Children's Hospital Medical Center.

Introduction

Membrane fusion is critical for the movement of molecules between cellular compartments, fertilization, development of multinucleated cells, and viral infection[1]. The fusion of two membranes is a mechanism by which cells and enveloped viruses facilitate entry into new domains, where cell-cell fusion results in the mixing of separate cellular contents into a syncytial cytoplasm, and virus-cell fusion leads to entry of viral genomes into cells. Membrane fusion is directly mediated by fusogens, which are a class of proteins that function to remodel membranes through diverse structural and biochemical mechanisms[2,3]. Given their function to drive entry of a virus into a cell, viral fusogens are employed in heterologous systems to control delivery of genetic or cellular material to cells. Indeed, VSV-G is the fusogen on vesicular stomatitis virus (VSV) and is utilized on other enveloped viruses to transduce a broad array of cell types in laboratory and clinical settings[4,5]. This process is called pseudotyping and has been used with structurally conserved fusogens from viruses, plants, and worms, to study fusion mechanisms and optimize viral targeting and transduction efficiencies[6–8]. Whether mammalian cell-cell fusogens that exhibit minimal homology to fusogens in other systems could substitute for viral fusogens and mediate fusion between viruses and cells is unknown.

Myomaker and Myomerger (also known as Myomixer/Minion) are the fusogens that control the fusion of progenitor cells to form multinucleated myofibers during skeletal muscle development and regeneration. Expression of these proteins is spatially and temporally controlled in muscle, where they are not present in quiescent satellite cells but are expressed exclusively in activated myogenic progenitors during fusion and then not expressed in mature myofibers. Myomaker and Myomerger are integral membrane proteins necessary for myoblast fusion, and their expression induces fusion in normally non-fusing cells[9–12]. However, Myomaker and Myomerger do not possess long extracellular domains typical of classical fusogens that could interact with the trans membrane. Instead, Myomaker exhibits homology to ceramidases[13] and Myomerger has characteristics similar to fusion-associated small transmembrane (FAST) proteins[14], and both muscle fusogens function on the cis membrane to modify the local environment and drive fusion through a unique mechanism[13,15], which remains to be fully deciphered. In addition, there are numerous cellular processes, including cell contact and actin nucleation, that cooperate with the myogenic fusogens to drive membrane coalescence in muscle cells[16]. Due to these multiple distinguishing characteristics, it is not intuitively obvious if the myogenic fusogens can function in systems devoid of parallel cellular activity. One barometer to evaluate the fusogenicity by Myomaker and Myomerger is to employ a cell-free system, such as engineered membranes, and assess their ability to replace viral fusogens.

Since the muscle fusogens function specifically in skeletal muscle, their inclusion on viral membranes may target the viruses to muscle. If Myomaker and Myomerger could modify tropism of enveloped viruses to skeletal muscle, it could aid in the delivery of therapeutic modalities. Correction of genetic muscle diseases, such as the muscular dystrophies, is a unique problem due to the distribution of muscle throughout the body in inaccessible locations[17]. Current approaches include gene restoration by Adeno-associated virus (AAV)[18,19], which exhibits tremendous efficacy in pre-clinical models but has not

yet achieved full clinical utility. In contrast, the development of therapeutic enveloped viruses has not progressed to be efficacious in pre-clinical models even though they possess desirable features including a larger packaging capacity, integration into genomes, transduction of stem cells, and potential for re-dosing[20]. Lentiviral vectors pseudotyped with viral fusogens can transduce dystrophic myofibers and muscle satellite cells, but the efficiency has been relatively low and systemic delivery has not been achieved due to an immune response against the viral pseudotypes[21–25]. The inability to target enveloped viruses specifically and efficiently to skeletal muscle remains the main obstacle for this class of delivery vehicle.

Here, we establish that Myomaker and Myomerger can drive fusion of basic membranes without the full complement of cellular machinery. As a result, we report the generation of a specialized class of enveloped viruses where Myomaker and Myomerger can functionally substitute for native viral fusogens and direct infectivity specifically towards myogenic targets for delivery of therapeutic material.

Results

Myomaker and Myomerger can be functionally pseudotyped on enveloped viruses and alter tropism

To investigate if Myomaker and Myomerger could drive fusion of viral membranes, we utilized a mutant form the vesicular stomatitis virus (VSV), a commonly used pseudotyping platform to assess the fusogenic function of a given protein[7,26]. The VSV genome was engineered with GFP (serving as a reporter for viral transduction) instead of the gene for the native G protein, which is responsible for viral membrane fusion (VSVΔG) (Figure S1A). Any fusion capability of VSVΔG must therefore be provided in trans by the membrane from the viral producing cells (Figure S1A)[7,26]. Studies using this system have shown that non-viral fusogens such as the *Caenorhabditis elegans* epithelial fusion failure 1 (EFF-1) and anchor cell fusion failure (AFF-1) proteins, which exhibit structural similarities to viral fusogens, can be used to generate infectious virions[7,8,27]. To facilitate incorporation of Myomaker and Myomerger on VSVΔG, we transduced BHK21 cell lines with either a control empty vector or vectors for both muscle fusogens, which can be regulated in a doxycycline-dependent manner (Figure S1B). After pelleting of virions from cell culture supernatants, we verified incorporation of the fusogens on viral membranes, along with VSV proteins within viruses, by immunoblotting (Figure S1C and S1D). VSVΔG virions from empty viral producing cells (Bald-VSVΔG) and Myomaker (Mymk) + Myomerger (Mymg) pseudotyped VSVΔG virions (Mymk+Mymg-VSVΔG) were first incubated with VSV-G antibodies to neutralize any remaining VSV-G activity then viruses were applied to BHK21 target cells that harbored an empty vector or expression cassettes for Myomaker and Myomerger. Transduction was not evident by Bald-VSVΔG on empty BHK21 cells although a non-statistically significant increase in GFP^+ cells was observed in recipient cells expressing Myomaker and Myomerger (Figure S1E and S1F). Mymk+Mymg-VSVΔG virions transduced BHK21 cells expressing Myomaker and Myomerger but not cells with empty vector (Figures S1E and S1F). To make certain that transduction observed by Mymk+Mymg-VSVΔG was due to the presence of Myomaker and

Myomerger and not residual VSV-G, we compared transduction with and without VSV-G neutralizing antibodies. Addition of neutralizing VSV-G antibodies blocked transduction by VSV-G-VSVΔG but not Mymk+Mymg-VSVΔG virions (Figure S1G). Mymk+Mymg-VSVΔG also transduced primary cultured mouse myotubes but not proliferating myoblasts or fibroblasts (Figure S1H). These data indicate that Mymk+Mymg-pseudotyped VSVΔG exhibits specific tropism towards cells expressing the muscle fusogens (myotubes and Myomaker + Myomerger expressing BHK21 cells).

Although we have demonstrated successful functional pseudotyping with Myomaker and Myomerger using the VSVΔG system, our ultimate goal is to exploit this hybrid platform towards engineering a safe and efficient muscle-targeting therapeutic vehicle. With multiple pitfalls precluding the use of VSV in a therapeutic setting most notably target cell toxicity[28] we utilized genome-integrating lentiviruses (LVs) (Figure 1A), another type of enveloped viruses but with greater clinical potential. We generated viral producing HEK293T cells with inducible expression of Myomaker and Myomerger (Figure 1B), and validated the presence of the muscle fusogens, and other viral components, on lentivirus particles produced from these cells (Figures 1C and 1D). Of note, Mymk+Mymg virions are devoid of VSV-G (Figure 1C). Transmission electron microscopy (TEM) analysis revealed relatively uniform rounded morphology of VSV-G pseudotyped lentivirus particles, and similar morphology in Mymk+Mymg virions (Figure 1E). We also performed immunogold EM for VSV-G, Myomaker, and Myomerger to confirm the presence of the fusogens on the lentiviral envelope. A single spot of intensity, corresponding to VSV-G, was observed on VSV-G pseudotyped particles (Figure 1F). For Mymk+Mymg virions, we utilized a dual detection system where secondary antibodies were conjugated to either 12nm (Myomaker primary antibodies) or 6nm (Myomerger primary antibodies) gold particles. This analysis confirmed presence of the muscle fusogens on LVs (Figure 1F). We next tested the transduction capacity of LVs pseudotyped with the muscle fusogens on empty and Myomaker + Myomerger-expressing BHK21 cells. Mymk+Mymg-LVs specifically transduced BHK21 cells expressing Myomaker and Myomerger, in contrast to the broad, non-specific tropism of VSV-G-LVs (Figure 1G). Titers obtained for Mymk+Mymg-LVs were comparable to VSV-G-LV titers (Figure 1H). We observed transduction by Mymk+Mymg-LVs on myotubes (~80%), low but statistically significant transduction in proliferating myoblasts, but no transduction in fibroblasts (Figure 1I). These findings demonstrate the feasibility for Myomaker and Myomerger pseudotyping on enveloped viruses, including those with therapeutic potential.

We next tested if both Myomaker and Myomerger are required on LVs for transduction by generating LVs with one or both of the muscle fusogens. Virions were produced at comparable levels for each pseudotype based on immunodetection of viral proteins from viral lysates and both Myomaker and Myomerger were independently incorporated on the virus without the need for the other fusogen (Figure S2A). LVs with one of the fusogens transduced Mymk+Mymg-expressing target cells at similar efficiencies, but there is an additive effect when both proteins were present on the viral membrane (Figures S2B and S2C). The ability for enveloped viruses pseudotyped with only one of the fusogens to induce virus-cell fusion suggests that both proteins are making independent contributions

on the virus. This is consistent with our previous finding where Myomaker and Myomerger function independently to make distinct contributions to the myoblast fusion reaction[15].

Since Myomaker and Myomerger endowed tropism of viral membranes for skeletal muscle cells, we asked if this effect was generalizable to other types of membrane-derived therapeutic vectors. We collected extracellular vehicles (EVs)[29] from 10T½ fibroblasts that overexpress Myomaker, Myomerger, or Myomaker and Myomerger (Figure S3A). Western blot analysis showed the presence of Myomaker and Myomerger on EVs (Figure S3B). EVs were labeled with the lipid probe DiI and placed on myotubes, where we observed significantly more uptake of EVs that contained one or both muscle fusogens (Figures S3C and S3D). These data show that the skeletal muscle fusogens could enhance tropism of non-viral membrane vectors to skeletal muscle cells.

Because Mymk+Mymg-EVs displayed tropism to myogenic target cells, and EVs are isolated from cell supernatants similar to LVs, we assessed if the the presence of EVs may be confounding outcomes in the Mymk+Mymg-LV transduction assays. In previous experiments, we isolated Mymk+Mymg-LVs by centrifugation (17,000 × *g*) to avoid pelleting of EVs, which are typically isolated by ultracentrifugation (100,000 × *g*). Nonetheless, we isolated Mymk+Mymg-LVs with centrifugation, ultracentrifugation, or purification of LVs with ultrcentrifugation over a sucrose cushion and compared levels of EVs and transduction. We found that overall protein amounts were lower with centrifugation (17,000 × *g*) and ultracentrifugation with a sucrose cushion (100,000 × *g*) compared to ultracentrifugation alone (Figure S3E). Similarly, the EV marker CD63 was absent with centrifugation and ultracentrifugation with a sucrose cushion (Figure S3E), indicating that ultracentrifugation alone pellets more material, including EVs, that could contaminate the LV prep. Moreover, concentration of Mymk+Mymg-LVs by ultracentrifugation alone resulted in the lowest transduction efficiencies (Figure S3F). Ultracentrifugation with a sucrose gradient (100,000 × *g*) also led to reduced transduction for both VSV-G-LV and Mymk+Mymg-LV compared to centrifugation (17,000 × *g*) (Figure S3F), which is consistent with reports that viral titers can be lost during purification steps. These data indicate that the observed transduction is specifically by fusion of Mymk+Mymg-LVs with target cells.

Myomaker and Myomerger pseudotyped lentivirus transduces skeletal muscle undergoing fusion

We next investigated if LVs pseudotyped with the muscle fusogens are capable of transducing muscle cells in vivo. LVs were chosen for in vivo analysis because approaches to package a genetic payload in EVs is difficult[30]. Since viruses pseudotyped with both muscle fusogens demonstrated maximum transduction efficiency in vitro, we generated Mymk+Mymg-pseudotyped lentivirus encoding Cre (Mymk+Mymg-LV-Cre). Viral supernatants were concentrated and 10^8-10^9 virions were injected into the tibialis anterior (TA) muscle of *Rosa*^{tdTomato} mice, which contains a Cre-dependent tdTomato cassette and serves as a readout for viral transduction (Figure 2A). The TAs of these mice were either uninjured or injured by cardiotoxin (CTX) four days prior to injection of the virus (Figure 2A). Two weeks following injection of Mymk+Mymg-LV-Cre, tdTomato$^+$

myofibers were observed in CTX-injured, but not in uninjured, muscle (Figure 2B). Here, we also utilized control Bald-pseudotyped (virions lacking a fusogen) lentiviruses encoding Cre and similar levels of virions were produced compared to Mymk+Mymg-LVs (Figure S2A), but no transduction in vivo was observed for Bald-LVs (Figure 2B). We also tested transduction in the synergistic ablation model (muscle overload)[31], which causes an increase in muscle load leading to induction of hypertrophy, and is comparatively less damaging than CTX injury but still induces activation and fusion of muscle satellite cells (Figure 2C). TdTomato^{+} myofibers were only detected in the plantaris muscle after muscle overload and injection with Mymk+Mymg-LV-Cre (Figure 2D). These data indicate that lentiviruses pseudotyped with Myomaker and Myomerger can transduce wild-type muscle in vivo when the muscle is stimulated and fusion occurs, such as following injury or a hypertrophic stimulus.

We next applied Mymk+Mymg-LVs to *mdx*^{4cv} mice, a model of Duchenne muscular dystrophy, which is a devastating genetic muscle disease resulting in chronic cycles of muscle injury and regeneration[32]. Bald- or Mymk+Mymg-LVs encoding Cre (10^{8}-10^{9} virions) were injected into the TA muscles of *mdx*^{4cv}; *Rosa*^{tdTomato} mice and viral transduction was assessed two weeks later (Figure 2E). Large areas of tdTomato^{+} myofibers were detected in muscles injected with Mymk+Mymg-LV-Cre without prior CTX injury, and the percentage of transduced myofibers increased after CTX (Figure 2F).

Mymk+Mymg-LVs can also deliver therapeutically relevant genetic material. We packaged a miniaturized form of the dystrophin gene (μDys5) that can partially compensate for full-length dystrophin[33], in Bald-LVs or Mymk+Mymg-LVs (Figure 2G). Viral particles were injected into TA muscles of *mdx*^{4cv} mice and analyzed 5 weeks later for μDys by immunohistochemistry. Consistent with the previous functional readout of reporter genes packaged by Mymk+Mymg-LVs in this study, we observed a wide distribution of myofibers expressing μDys while no such expression was detected in muscle treated with Bald-LVs (Figures 2H and 2I). Western blot analysis confirmed expression of μDys in muscle 6 months after intramuscular delivery of Mymk+Mymg-LV-μDys (Figure 2J). Taken together, these results highlight that after local injection, Mymk+Mymg-pseudotyped virus can transduce dystrophic skeletal muscle cells.

Myogenic progenitors are targeted by Mymk+Mymg-pseudotyped lentiviruses

Since we observed an increase in tdTomato^{+} myofibers in settings when myogenic progenitors are activated (injury, muscle overload, dystrophic muscle), we postulated that Mymk+Mymg-LVs may be trophic for myogenic progenitors. We assessed tdTomato expression in α7-Integrin^{+} myogenic cells five weeks following intramuscular injection of pseudotyped LVs in TA muscles of *mdx*^{4cv}; *Rosa*^{tdTomato} mice. Standard FACS analysis was used to identify the α7-Integrin^{+} cells (Figure S4)[34], and revealed that ~50% of α7-Integrin^{+} cells were positive for tdTomato following Mymk+Mymg-LV-Cre but not Bald-LV-Cre administration (Figure 3A). Indicating specificity of Mymk+Mymg-LVs for myogenic cells, the number of tdTomato^{+} non-myogenic cells was negligible (Fig. 3A). In a separate experiment, we generated Mymk+Mymg-pseudotyped lentivirus encoding luciferase (Luc) and compared its transduction capacity to VSV-G-pseudotyped lentivirus

following intramuscular injection of CTX-injured *mdx*^{4cv} TA muscles (Figure 3B). Luciferase activity was significantly higher in TA muscles injected with Mymk+Mymg-LV-Luc as compared to those injected with VSV-G-LV-Luc one week following viral injections (Figure 3B). Moreover, time course analysis revealed an increase in bioluminescence in Mymk+Mymg-LV-Luc treated animals over time (Figure 3B). We interpret the increase in luciferase signal over time to be contributed by the ongoing fusion of transduced muscle satellite cells. To test if the genetic payload delivered by Mymk+Mymg-LVs indeed modifies the satellite cell pool of recipient muscles, we injured *mdx*^{4cv}; *Rosa*^{tdTomato} muscles that were previously transduced by Mymk+Mymg-LV-Cre (Figure 3C). We observed tdTomato^{+} myofibers after injury (Figure 3C), indicating that the genetic material delivered by Mymk+Mymg-LV-Cre is present in satellite cells needed for regeneration after injury. These results highlight that after local injection, Mymk+Mymg-pseudotyped virus can transduce myogenic progenitors.

Myomaker in target cells is required for fusion with viruses pseudotyped with the muscle fusogens

For efficient fusion of myoblasts to initially form a nascent myofiber, Myomaker is required on both cells and Myomerger is needed on one cell[11,35]. Extrapolation of this myoblast fusion model to the virus-cell fusion platform described here would predict that Myomerger would not function alone on viruses to allow entry into target cells expressing both fusogens. However, we find that Myomaker and Myomerger can function alone on virions to drive fusion with target cells (Figure S2) suggesting that virus-cell fusion may have different requirements. Thus, we investigated the requirements of the muscle fusogens in target cells for fusion with viruses, information that could aid in the design of a system to optimize cell-type specific tropism. Mymk+Mymg-pseudotyped LVs were applied to empty, Myomaker, Myomerger, or Myomaker and Myomerger BHK21 cells. Target cells expressing Myomaker or Myomaker and Myomerger, but not Myomerger alone, were transduced by Mymk+Mymg-pseudotyped LVs indicating a necessity for Myomaker on target cells (Figure 4A). These data indicate a critical function for Myomaker on the target cell for viral receptivity in this specialized system.

We next explored if Myomaker was also required in recipient dystrophic muscle tissue for transduction by Mymk+Mymg-LV-μDys. We genetically deleted Myomaker from muscle progenitors in the dystrophic background (*mdx*^{4cv}; *Mymk*$^{loxP/loxP}$; *Pax7*^{CreER}) and then intramuscularly delivered Mymk+Mymg-LV-μDys (Figure 4B). Loss of Myomaker-expressing fusogenic cells resulted in a lack of transduction by Mymk+Mymg-LV-μDys (Figure 4B), indicating that the availability of Myomaker^{+} recipient cells in the tissue at the time of LV delivery is one of the determining factors for efficacious transduction.

Myomaker + Myomerger pseudotyped LVs evade a neutralizing immune response

An important consideration for a delivery vehicle is an ability to specifically transduce muscle after systemic delivery. Since our data indicate that Mymk+Mymg-LVs target Myomaker^{+} fusogenic cells, and it is well established that both the expression of Myomaker and levels of activated myogenic progenitors are transient in dystrophic muscle[36,37], the number of recipient cells available for transduction at any given time can be limiting. Thus,

we may need multiple timely doses of Mymk+Mymg-LVs to efficiently target skeletal muscle. However, re-dosing animals with the same gene therapy vector, such as current muscle trophic vectors like AAV9, is challenging due to development of a neutralizing immune response to the initial dose[38]. We tested if there is a similar neutralizing immune response to Mymk+Mymg-LVs by sequential intramuscular delivery of Mymk+Mymg-LV-Cre or AAV9-Cre into *mdx*^{4cv}; *Rosa*^{tdTomato} mice. Mymk+Mymg-LV-Cre, but not AAV9-Cre, transduces the right TA despite prior exposure to the virus when the contralateral (left) TA was transduced 4-weeks earlier (Figure S5A), indicating that Mymk+Mymg-LVs do not elicit a neutralizing immune response at a level that precludes re-dosing.

We also tested a systemic dosing strategy by adjusting the amount of Mymk+Mymg-LVs and number of doses. Mymk+Mymg-LV-μDys was administered through a single retro-orbital (RO) injection to *mdx*^{4cv} mice at 4 weeks of age, which is a timepoint when muscle pathology is active and fusogenic muscle progenitors should be present (Figure S5B)[36]. One cohort of mice was treated with Mymk+Mymg-LV-μDys at an approximate titer of 10^9 and a separate cohort received 10^{10} virions (Figure S5B). At 8 weeks of age, we sacrificed the animals and assessed μDys levels in the diaphragm by immunostaining, and found 34% μDys$^+$ myofibers with 10^9 virions and 47% with 10^{10} virions (Figure S5B). We selected the dose of 10^9 to evaluate the timing of delivery and dosing frequency since that dose was efficacious and it is ideal to use the lower titers for gene therapy strategies to avoid potential off-target deleterious consequences. To assess if re-dosing systemically resulted in an improved transduction, we delivered Mymk+Mymg-LV-μDys through two successive RO doses delivered two weeks apart. Here, we found 63% μDys$^+$ myofibers in diaphragms when Mymk+Mymg-LV-μDys was re-dosed (Figure S5C). Finally, we treated *mdx*^{4cv} mice with three successive doses of Mymk+Mymg-LV-μDys and decided to administer the extra dose at 2 weeks of age (Figure S5D) because the number of activated myogenic progenitors available for transduction is higher at earlier postnatal timepoints[36]. This dosing regimen yielded the 78% μDys$^+$ myofibers (Figure S5D) in diaphragms, which is the most efficacious transduction compared to the other strategies attempted. The number of μDys$^+$ myofibers positively correlating with the number of Mymk+Mymg-LV-μDys doses delivered systemically is consistent with our findings that the availability of Myomaker$^+$ recipient cells is a determining factor for transduction. Moreover, the increased transduction after multiple systemic doses confirms immune evasion by Mymk+Mymg-LV-μDys, which is in contrast to any current therapeutic LVs such as VSV-G-LV that are inefficient in transduction of most tissues including skeletal muscle following systemic delivery, likely due to its neutralization by an activated immune response towards VSV-G[24].

Myomaker and Myomerger pseudotyped lentivirus specifically transduces skeletal muscle following systemic delivery

We determined the specificity of Mymk+Mymg-LVs and assessed potential variability of delivery to different muscle groups. We evaluated tdTomato labeling in non-muscle and skeletal muscle tissues following systemic delivery of Bald- or Mymk+Mymg-LV-Cre (10^9 virions) to *mdx*^{4cv}; *Rosa*^{tdTomato} mice. LVs were administered to mice through three retro-orbital injections starting at two-weeks of age and multiple tissues were analyzed two weeks after the final injection (Figure 5A). We observed viral transduction in all skeletal

muscles analyzed by Mymk+Mymg-LV-Cre but not Bald-LV-Cre (Figures 5B and 5C). Notably, we observed maximum and robust transduction in the diaphragm muscle (~80% of myofibers) (Figures 5B and 5C), which is critical to target since respiratory failure is a major reason for mortality in many skeletal myopathies[39]. We observed transduction of approximately 10% of myofibers in the limb muscles (Figure 5C). Moreover, we did not detect evidence of viral transduction in non-skeletal muscle tissues including heart, kidney, liver, and spleen (Figure 5D), highlighting the specificity of this pseudotyped vehicle. The lack of transduction in non-muscle tissues is expected given the absence of Myomaker and Myomerger expression and cellular fusion in those tissues. Altogether, these findings are supportive of a skeletal muscle-specific targeting role for systemically delivered Mymk+Mymg-pseudotyped viruses.

Systemically administered Myomaker and Myomerger pseudotyped lentivirus delivers therapeutic material to dystrophic muscle and alleviates pathology

We next tested if μDys delivered by Mymk+Mymg-LVs through three doses of systemic retro-orbital injections was sufficient to reduce muscle pathology in dystrophic animals (Figure 6A). For mice treated with Mymk+Mymg-LV-μDys, μDys was detected two weeks after the final injection in 5–25% of myofibers in limb muscles (Figure S6A and S6B) and 77–90% of myofibers in the diaphragm (Figure 6B and 6C). Mymk+Mymg-LVs delivered enough μDys to the diaphragm to reduce indices of pathology including centrally nucleated myofibers (Figure 6D) and fibrosis (Figures 6E and 6F). μDys was detected by western blot in diaphragms 2 weeks after treatment with Mymk+Mymg-LV-μDys but not Bald-LV-μDys (Figure S6C), and this level corresponded to an average of 114% of total normal dystrophin levels in wild-type diaphragms (Figure S6D). We also determined the long-term consequences on dystrophin expression, muscle function, and membrane permeability after treatment with Mymk+Mymg-LV-μDys. 6 months after delivery of the LVs, mice were injected with Evan's blue dye (EBD) and muscle contraction and dystrophin levels were analyzed (Figure 6G). We found 30% of gastrocnemius myofibers were positive for μDys 6 months after treatment (Figure S6E), which is an increase compared to 13% μDys^+ myofibers 2 weeks after treatment (Figures S6A and S6B). EBD is typically excluded from cells with intact plasma membranes, but the dye can enter dystrophic myofibers due to an unstable sarcolemma. In diaphragm muscles, we observed reduced EBD^+ myofibers in animals treated with Mymk+Mymg-LV-μDys indicating a stabilized sarcolemma (Figure 6H). Moreover, diaphragm muscles that received Mymk+Mymg-LV-μDys also produced increased specific force compared to dystrophic diaphragms treated with Bald-LV-μDys (Figure S6F). Gastrocnemius muscles from mice treated with Mymk+Mymg-LV-μDys also exhibited an increase in specific force (Figure 6I) and were protected from force loss after repeated eccentric contractions (Figure 6J), a hallmark endpoint for assessment of therapeutic efficacy. Consistent with improved force generation, gastrocnemius muscles exhibited fewer EBD^+ myofibers at baseline and after repeated eccentric contractions (Figure 6K) indicating a stabilized sarcolemma. Overall, these results provide proof-of-concept experimental evidence for the therapeutic utility of enveloped viruses pseudotyped with the muscle fusogens.

Discussion

The muscle-specific proteins Myomaker and Myomerger drive the final steps of skeletal muscle cell fusions. The work described in this study addressed two main questions: a) can Myomaker and Myomerger drive fusion of cell-free membranes and if so, b) can the muscle-specific fusogens direct tropism of non-cellular membranes towards myogenic cells. These questions needed to be investigated and answered because it was unclear whether the functional properties of the muscle fusogens to modulate the cis membrane could be transferred to cell-free membranes like viral membranes and substitute for native viral fusogens that act on the trans membrane. The pseudotyping results shown here advance our understanding of these fusogens as they confirm the ability of Myomaker and Myomerger to function in the absence of additional cellular processes implicated in muscle cell-cell fusion. We anticipate this pseudotyping platform, where the individual activity of each of the muscle fusogens can be isolated will be utilized in future studies to better understand cell fusion mechanisms.

To the best of our knowledge, this study is the first to report the generation of a viral vector pseudotyped with mammalian fusogens that can function as a therapeutic delivery vehicle for a specific cell-type. Mymk+Mymg-LVs overcome a major obstacle in lentiviral gene therapy for muscle and adds to potential approaches to correct muscle diseases either alone or in combination with current viral-based gene therapies. Lentiviral vectors have been the subject of decades of research[4,22,40,41] due to desirable features like genomic integration, relatively large packaging capacity, and transduction of stem cells which makes them a promising vector for potential lifelong supply of an absent or defective protein. Despite these desirable qualities, their therapeutic application has been hindered due to a reliance on viral pseudotypes, such as VSV-G, that are neutralized by the complement system upon systemic delivery[42]. Another general concern for LV-based therapy is oncogenesis due to random insertion into the genome[43,44], but this may not be an issue since there are methods to bias integration[45]. Thus, the unique advantages of Mymk+Mymg-LVs have the potential to circumvent some enduring challenges associated with AAV gene therapy, which currently dominates gene-corrective strategies for muscle. AAV gene therapy has potential issues including pre-existing immunity, toxicity, off-target effects, dosing-limitations, and limited transgene persistence[46–49], indicating that alternative vectors need to be developed.

A major issue with gene and cell therapies is an ability to deliver material specifically to the tissue of interest. We establish that vectors pseudotyped with the muscle fusogens are highly specific for skeletal muscle cells after local and systemic delivery. Systemically injected Mymk+Mymg-LVs into dystrophic mice target all skeletal muscle tissues analyzed at varying efficiencies. 5–25% of myofibers in limb muscles expressed μDys two weeks after the final injection of Mymk+Mymg-LV-μDys, with mean protein levels exceeding 100% of wild-type levels in diaphragms. Consistent with dystrophic myofibers expressing μDys after treatment with Mymk+Mymg-LV-μDys, we observed a reduction in pathologic indices such as reduced central nucleation and fibrosis, and an improvement in functional parameters.

Tropism of any vector not only depends on the components on the surface of the vector but also factors on recipient cells, therefore we investigated the determinants in recipient cells for transduction by Mymk+Mymg-LVs. In vitro, transduction is sufficient when Myomaker is present in non-muscle target cells and in vivo transduction by Mymk+Mymg-LVs is restricted to skeletal muscle conditions associated with activated and differentiating muscle progenitors that express the muscle fusogens. These data overall suggest that the cell type in muscle that is transduced in vivo is one which expresses the muscle fusogens, and we show that Myomaker is required. In dystrophic muscle, Myomaker is expressed in activated muscle progenitors derived from satellite cells and regenerating myofibers that exhibit Myomaker expression contributed from the fusion of progenitors[37]. The need for Myomaker in target cells explains why uninjured wild-type muscle is not transduced since there are no Myomaker-expressing activated progenitors or regenerating myofibers[10], and also likely explains increased transduction efficiencies in muscles like the diaphragm that exhibits elevated and sustained levels of fusion of myogenic progenitors[50].

Targeting activated muscle progenitors by Mymk+Mymg-LVs raises the possibility that this pseudotyping approach affords the opportunity to permanently modify the resident satellite cell population, which could offer a supply of therapeutically corrected cells that can continue to fuse with myofibers over the lifetime of the recipient. Indeed, the presence of transduced muscle progenitors five weeks after intramuscular viral delivery, the increase in luciferase signal in myofibers after 11 months, and the presence of transduced myofibers following re-injury, strongly suggest that satellite cells are modified. Since we do not observe transduction in wild-type muscle, it is unlikely that Mymk+Mymg-LVs directly transduce quiescent satellite cells. We anticipate that modification of the satellite cell pool results from transduction of activated progenitors by Mymk+Mymg-LVs that then undergo self-renewal and revert to quiescence[51]. While the ability for Mymk+Mymg-LVs to transduce differentiating muscle progenitors allows specificity and could result in modification of the stem cell compartment, these characteristics of the system are also a limitation because the presence of Myomaker-expressing progenitors or regenerating myofibers fluctuate in mouse dystrophic muscle depending on whether the muscle is undergoing degeneration or regeneration. There is an even greater lack of knowledge about levels of myogenic progenitors, and Myomaker and Myomerger expression, in normal and dystrophic human muscle tissue. Thus, it remains to be determined if this platform could be utilized for a wider range of genetic and acquired myopathies that do not manifest in muscle injury that elicits activation of satellite cells.

The precise delivery modalities for lifelong correction of genetic muscle diseases cannot be currently ascertained. Non-enveloped viral vectors like AAV9 and Myo-AAV exhibit more robust transduction, compared to Mymk+Mymg-LVs, after a single dose[18,33] because the vector is highly trophic for mature myofibers that are always present in normal and dystrophic muscle. Another advantage of AAV is that they target cardiac tissue, which is a critical component of pathology in many diseases such as Duchenne muscular dystrophy. However, AAV serotypes may be difficult to re-dose due to the development of a neutralizing immune response to the vector. We show that Mymk+Mymg-LVs can be re-dosed, which allows for increased targeting of permissive cells present in the dystrophic environment at various timepoints, and also demonstrates that the LVs exhibit immune

evasion. But Mymk+Mymg-LVs do not target cardiac tissue thus could only be used as a stand-alone approach in therapies for muscle diseases not affecting the heart, such as X-linked myotubular myopathy. In genetic diseases involving both skeletal and cardiac muscles, we propose that two vectors could be used in combination. One could envision that Mymk+Mymg-LVs are used to target progenitor cells and regenerating myofibers when the availability of those cell types are high in skeletal muscle, then AAVs could be used to further elevate dystrophin expression in mature myofibers and cardiac cells. Overall, our findings demonstrate that the fusogenic properties of mammalian muscle fusogens can be transferred to viral membranes thus establishing a specialized class of delivery vehicles that are specific for skeletal muscle.

Limitations of the Study

The data presented here show that Mymk+Mymg-LVs have biological and therapeutic potential especially considering this is the first description of a delivery vehicle that harnesses the muscle-specific fusion machinery to drive tropism. Nonetheless, there are many questions raised by the findings related to the mechanism of homing and entry of Mymk+Mymg-LVs, the full repertoire of determinants in recipient cells that will inform situations for which the pseudotyped LVs could be used, and potential scalability. The study did not illuminate mechanisms by which the virus infects cells and this usually occurs through fusion events either at the cell surface or in intracellular compartments following endocytosis[52]. It is also important to note that enveloped virions and extracellular vesicles utilized in this study are cellular products and we cannot exclude the possibility that cellular events mediated by Myomaker and Myomerger catalyze a fusion-favorable membrane prior to viral or extracellular budding. Therefore, it remains to be determined if the muscle fusogens can bestow fusion to synthetic membranes devoid of any prior cellular activity. Comprehensive molecular characterization of the pseudotyped virions will be an investigative goal.

We expect the foundational therapeutic vehicle described in this study can be further optimized with additional proteins and lipids as mechanistic details of the myoblast fusion reaction are uncovered. A critical question not evaluated is the biodistribution of Mymk+Mymg-LVs and since lentiviruses in general are inefficient after systemic delivery[53], this process could be limiting for Mymk+Mymg-LVs and it would represent a pathway for further engineering. Moreover, non-viral membrane vehicles, such as extracellular vesicles containing Myomaker and Myomerger, could be utilized as also shown in this study. Finally, while we demonstrate proof-of-concept for the therapeutic utility of lentiviruses pseudoytuped with the muscle fusogens, we recognize that the translatability of this gene delivery vehicle requires rigorous assessment of various parameters such as toxicity, oncogenicity, and scaling of vector production, all of which, need to be evaluated in following studies.

STAR METHODS

RESOURCE AVAILABILITY

Lead Contact—Please direct request for resources and reagents to Lead Contact: Douglas P. Millay (douglas.millay@cchmc.org)

Materials Availability—Plasmids and cell lines generated in this study are available upon request. Signing a materials transfer agreement (MTA) may be required. All data are available in the main text or supplementary materials.

Data and Code Availability—This study did not generate original code or sequencing data. Any additional information related to the data in the manuscript is available from the lead contact.

EXPERIMENTAL MODEL AND SUBJECT DETAILS

Animals—All mice used in this study were maintained on a C57BL/6 background including C57BL/6 (wild-type), *mdx*^{4cv} (stock #002378; The Jackson Laboratory, Bar Harbor, ME, USA), *Rosa26*^{tdTomato} (stock #007905; The Jackson Laboratory). *Mdx*^{4cv}; *Rosa26*^{tdTomato} mice were generated by crossing *mdx*^{4cv} mice with *Rosa26*^{tdTomato} mice. *Myomaker*$^{loxP/loxP}$; *Pax7*^{CreER} mice (Mymk^{scKO}) mice used in this study were described previously[57]. Tamoxifen (75 mg/kg body weight) dissolved first in ethanol then in corn oil was administered to mice through intraperitoneal injection. All experiments were performed on gender- and age-matched cohorts, where both male and female mice were used, and animals were randomly assigned to control or experimental groups. All animal procedures were approved by Cincinnati Children's Hospital Medical Center's Institutional Animal Care and Use Committee and were conducted in accordance with Association for Assessment and Accreditation of Laboratory Animal Care International guidelines.

Cells—Primary myoblasts were isolated from wild-type mice as described previously[58]. Cells were plated on matrigel-coated plates, maintained in growth medium (20% fetal bovine serum (Peak Serum) and 2.5 ng/ml human bFGF (PeproTech) in Ham's F-10 nutrient mixture (Gibco or Cytiva) with penicillin/streptomycin (Gibco), and differentiated in differentiation media (2% horse serum (Gibco) in high-glucose DMEM (Gibco or Cytiva), with penicillin/streptomycin). 10T½ fibroblasts were purchased from American Type Culture Collection and propagated in DMEM (Gibco or Cytiva) containing 10% heat-inactivated fetal bovine serum and supplemented with antibiotics and sodium pyruvate (Gibco). HEK293T and C2C12 cells were purchased from American Type Culture Collection (ATCC), and Baby hamster kidney (BHK21) cells were provided by Dr. Michael Whitt. Cells were propagated in DMEM (Gibco or Cytiva) containing 10% heat-inactivated fetal bovine serum and supplemented with antibiotics along with sodium pyruvate for HEK293T and BHK21 cells and L-glutamine (Gibco) for BHK21 cells. All doxycycline inducible expression cell lines were propagated in DMEM containing 10% Tet-Free fetal bovine serum (Peak Serum). Platinum-E retroviral packaging cells were purchased from Cell Biolabs and propagated under constant selection conditions in DMEM (Gibco) containing

10% heat-inactivated fetal bovine serum and supplemented with antibiotics and sodium pyruvate. All cells were grown and maintained in a 37°C incubator with 5% CO_2.

METHOD DETAILS

Traditional (VSV-G-pseudotyped) lentivirus generation—5×10^6 HEK293T cells were plated on a 100 mm dish and transfected with a cocktail of 10 μg transfer plasmid, 7.5 μg psPAX2 packaging plasmid (Addgene, plasmid #12260), and 2.5 μg pMD2.G envelope plasmid (Addgene, plasmid #12259) with 60 μl FuGENE-6 (Promega Madison, WI, USA) or polyethylenimine (PEI) (linear, MW 250,000) (Polysciences Warrington, PA, USA) or in 1ml DMEM. For experiments using PEI, media was changed after 4h and supernatant containing viral particles was collected 40–48h later. For viral preparation utilizing FuGENE-6, no media change was performed and supernatant containing viral particles was collected 48h later. Viral supernatants were centrifuged at 2500 rpm for 2.5 minutes and passed through a 0.45 μm SFCA filter before use. For lentivirus utilized in generating viral producing BHK21 and HEK293T cells, mouse Myomaker, mouse Myomerger, EFF1-V5, were cloned into the transfer lentivirus plasmid pLVX-TetOne-Puro (Clontech, plasmid #631849) or pLVX-TetOne-Blast (modified from Clontech, plasmid #631849).

Retrovirus generation—5×10^6 Platinum-E retroviral packaging cells (Cell Biolabs, San Diego, CA, USA) were transfected with a cocktail of 10 μg of pBabe-X-Myomaker and/or pBabe-X-Myomerger, or pBabe-X-empty plasmid along with 30 μl FuGENE-6 in DMEM. After 48 hours, supernatants containing retroviral particles were centrifuged at 2500 RPM for 2.5 minutes and passed through a 0.45 μm SFCA filter before use.

Myomaker, Myomerger, EFF1-V5 pseudotyped viral producing and recipient cell lines—Baby hamster kidney (BHK21) cells were transduced with lentivirus coding for doxycycline-inducible Myomaker and/or Myomerger, EFF1-V5, or an empty cassette to generate cells that would produce pseudotyped VSV. BHK21 cell lines generated here were also used as viral recipient cells in this study. For generation of lentiviral producing cell lines with various pseudotypes, HEK293T cells were transduced with traditional VSV-G pseudotyped lentivirus coding for doxycycline inducible Myomaker and/or Myomerger, or empty plasmid. Transduction of both BHK21 and HEK293T cells to express the fusogen (Myomaker and/or Myomerger, or EFF1-V5) was achieved through spinfection by centrifugation at 600 × *g* for 1 hour at 22°C immediately following viral overlay and incubated overnight. Cells were then selected with puromycin or blaticidin for 72 hours.

The above BHK21 cells were used as recipient cells for assessment of function and titering. For Cre-coding lentiviral pseudotypes, BHK21 recipient cells were generated by initial transduction with traditional VSV-G lentivirus coding for a Cre-reporter (plasmid #62732, Addgene, Watertown, MA, USA), followed by transduction with empty or doxycycline inducible Myomaker + Myomerger -lentivirus (traditional VSV-G pseudotyped) in a manner as described above.

Extracellular vesicle producing cells—10T½ fibroblasts were transduced with retrovirus generated from platinum E cells which were transfected with pBabeX-Myomaker and/or pBabeX-Myomerger, or pBabeX-empty. Fibroblasts were subjected to spinfection by centrifugation at 600 × *g* for 1 hour at 22°C immediately following viral overlay and incubated overnight.

Generation of pseudotyped vesicular stomatitis virus—0.5×10^6 Myomaker and/or Myomerger, EFF-1-V5, or empty BHK21 cells (all dox-inducible) were selected with puromycin, then plated on a 60 mm cell culture plate with 250 ng/ml doxycycline for 36 hours. Cells were then infected with VSVG-complemented VSVΔG recombinant virus (VSVΔG-G) for 2 hours in serum free DMEM. Virus infected cells were washed 3 times with PBS to remove unabsorbed VSVΔG-G virus. Following a 24-hour incubation, the supernatant containing the VSVΔG-pseudovirus was harvested and centrifuged twice at 2500 RPM for 5 minutes to remove cellular debris. Pseudotyped viral supernatants were then treated with anti-VSV-G (1:1000, #8G5F11, Kerafast) to neutralize any residual VSV-G. Viral supernatants were either immediately used for functional analysis or concentrated by ultracentrifugation for detection of fusogenic proteins on viral particles. For functional analysis, VSV pseudotypes were applied to modified BHK21 cell lines as described below (viral titering section).

Generation of lentivirus pseudotyped with the muscle fusogens—2.5×10^6, 5×10^6, or 10×10^6 Myomaker and/or Myomerger, or empty inducible HEK293t cell lines generated in this study were plated on 60-, 100-, or 150-mm dishes respectively. After 24 hours, cells were then treated with 1 μg/ml doxycycline for 2 hours after which media was changed to 100 ng/ml doxycycline in 2% horse serum in DMEM. Cells were then transfected with a cocktail of lentivirus transfer plasmid (5, 10, or 20 μg) along with lentiviral packaging plasmid (3.75, 7.5, or 15μg psPAX2) and FuGENE-6 (Promega) or PEI (Polysciences) at a ratio of 1:3 μg DNA:μl transfection reagent in DMEM. We obtained lentiviral transfer plasmids encoding for GFP, μDystrophin, Cre, and Luciferase by sub-cloning or they were purchased. GFP and μDystrophin were inserted into a pLX304 vector (Addgene, Plasmid #25890), where pLX304-GFP[56] was generated previously and μDystrophin was cloned into pLX-304 after excision from pAAV-CK8e-ChimericIntron-hDys5coGA-synPA[33]. We replaced eGFP in pLKO.1-puro eGFP (Sigma Aldrich, plasmid #SHC005) with Cre through standard cloning techniques. The Luciferase plasmid was directly purchased from Addgene (pLX304-Luciferase-V5 (Addgene, plasmid #98580)). After 16–24 hours, viral supernatants were collected, cellular debris was cleared, and passed through a 0.45 μm SFCA filter and either immediately used for functional analysis, concentrated by centrifugation at 17,000 × *g* or 100,000 × *g*, or stored at −80°C for later use. Remaining cells were replenished with fresh 2% horse serum in DMEM supplemented with 50 ng/ml doxycycline for another 16–24 hours where a second collection of viral supernatants was performed and processed as described for the first viral supernatant collection.

Lentiviral purification—Lentiviral purification was performed by the CCHMC Viral Vector Core. Briefly, 30–32ml of Bald-, VSV-G-, or Myomaker+Myomerger-pseudotyped

viral supernatants were centrifuged for 5 minutes at 2,500 RPM to clear cellular debris and passed through a 0.45 μm SFCA filter. Viral supernatants were then overlayed on 5–6ml of 20% sucrose and centrifuged for 90 minutes at 100,000 × *g* at 4°C. Finally, viral pellets were resuspended in 100μl of PBS by gentle rocking for 1 hour.

Functional assessment of pseudotyped virus in myogenic and non-myogenic cells—Primary myoblasts, myotubes, or 10T½ fibroblasts were plated on 48-well cell culture plates and overlayed with pseudotyped VSVs or LVs coding for GFP with 6 μg/ml polybrene and subjected to spinfection as described above. Viruses were added directly to the normal culturing media for each cell type. After 12–16 hours, media was replaced and cells were incubated for another 24 hours for cells transduced with VSV-pseudotypes, and 48 hours for those transduced with LV pseudotypes. Cells were then fixed with 2% paraformaldehyde (PFA, #43368–9M, Alfa Aesar) and stained with Alexa Fluor 546-conjugated phalloidin (A22283, Invitrogen) and Hoechst (#H3570, Molecular Probes). GFP expression in cells served as a readout for viral transduction.

Viral titering—To determine functional titers of viral pseudotypes, 1×10^3 or or 1×10^4 empty BHK21 cells or those expressing dox-inducible Myomaker and/or Myomerger, or EFF-1 (with or without Cre-reporter) were plated in each well of a 96-well or a 12-well tissue culture plate, respectively. These cells were plated with 500 ng/ml doxycycline. 24 hours later, cells were overlayed with serial dilutions of VSV or LV pseudotypes with 6 μg/ml polybrene and subjected to spinfection by centrifugation at 600xg for 1 hour at 22°C. For VSV pseudotypes, viral titers were determined 24 hours following transduction where cells were fixed with 2% PFA and stained with Hoechst, followed by quantification of GFP^+ cells using the Cytation™ 5 (BioTek, Winooski, VT, USA). For lentiviral pseudotypes, media was changed 16–18 hours following transduction and cells were analyzed 24 hours later. Cells were fixed with 2% PFA and stained and imaged or trypsinized and GFP^+ cells were counted using the Countess 3 Automated Cell Counter (Invitrogen, Waltham, MA, USA). Viral titers were then determined using the following formula TU/mL = (Number of cells transduced × Percent fluorescent × Dilution Factor)/(Transduction Volume (mL)).

Preparation and labeling of extracellular vesicles—Culture media of 10T½ fibroblasts overexpressing Myomaker and/or Myomerger or empty plasmid was collected following two days in exosome-depleted serum and sequentially centrifuged at 1000 × *g* for 10 minutes then 10,000 × *g* for 30 minutes. The supernatants were collected and passed through a 0.22-mm filter (Corning, Corning, NY, USA), followed by ultracentrifugation at 100,000 × *g* at 4°C overnight. Extracellular vesicle pellets were washed with cold PBS and recovered by ultracentrifugation at 100,000 × *g* for 3 hours. For protein detection on extracellular vesicles, pellets were lysed in NP-40 lysis buffer and further processed for immunoblotting.

Functional assessment of Myomaker and Myomerger coated extracellular vesicles—Extracellular vesicle (EV) pellets were resuspended in PBS following final ultracentrifugation and equal concentrations of extracellular vesicle were labeled with lipophilic membrane stain (1,1’-Dioctadecyl-3,3,3’,3’-Tetramethylindocarbocyanine

Perchlorate (‘DiI’; DiIC18(3)). EVs were washed one time with PBS to remove unincorporated DiI. 5 μg of DiI-labeled EVs were overlayed onto primary myotubes in 8-well chamber slides in corresponding culturing media for 12 hours. Cells were then washed twice with DMEM and replenished with fresh culturing media. 12 hours later, cells were fixed with 2% PFA, stained with Hoechst to label nuclei, and analyzed for DiI fluorescence as a readout of extracellular vesicle uptake.

In vivo viral delivery—Bald, VSV-G, or Myomaker + Myomerger-pseudotyped lentivirus coding for Luciferase, Cre, or μDystrophin was prepared as described above. For intramuscular injections, 40–80 mL of viral supernatant (per muscle) was first centrifuged for 5 minutes at 2,500 RPM to clear cellular debris and passed through a 0.45 μm SFCA filter. Supernatants (containing the virions) were then concentrated by centrifugation at 10,000 RPM at 4°C for at least 4 hours. The viral pellet was washed once with PBS followed by centrifugation at 10,000 RPM at 4°C for at least 4 hours. The viral pellet was finally resuspended in 25–40 μl PBS and injected into the tibialis anterior or plantaris muscle of the indicated mice using an insulin syringe equipped with a 28-gauge needle. For retro-orbital injections 100–1000 ml of viral supernatant (per mouse) was concentrated as mentioned above. The viral pellet was finally resuspended in 60–100 μl PBS and injected retro-orbitally by the Cincinnati Children’s Hospital Medical Center Comprehensive Mouse and Cancer Core. Some cohorts of mice were subjected to cardiotoxin-induced muscle injury or muscle overload prior to or after delivery of pseudotyped lentivirus. 35 μl of 10 μM stock of cardiotoxin (EMD Millipore Cat. #217503) was injected into the tibialis anterior muscle and viral injections were administered 4 days later. For experiments described in Figure 3C, cardiotoxin was injected into the tibialis anterior muscle 2 weeks following viral administration. Overload of the plantaris muscle was achieved through bilateral synergist ablation of the soleus and gastrocnemius muscles of 3-month-old mice. Briefly, the gastrocnemius muscle was exposed by making an incision on the posterior-lateral aspect of the lower limb. The distal and proximal tendons of the soleus, lateral and medial gastrocnemius were subsequently cut and carefully excised. Viral injections were administered to plantaris muscle 7-days following surgery. For assessment of viral immune neutralization in vivo, AAV9-Cre (#105537, Addgene), Bald-LV-Cre, or Mymk+Mymg-LV-Cre were injected into the left TA muscle of (4–5)-week old *Mdx*^{4cv}; *Rosa26*^{tdTomato} mice and 28 days later the same viral species were injected into the right TA of the same cohort of mice and muscle were harvested after 28 days and processed for histological analysis.

Immunoblotting—Cell, viral, or extracellular vesicle pellets were lysed in NP-40 lysis buffer (50 mM Tris-Cl (pH 8.0), 200 mM NaCl, 50 mM NaF, 1 mM dithiotheritol, 1 mM sodium orthovanadate, 1 mM Benzamidine, 0.3% NP-40 and protease inhibitors). Lysates from cells or extracellular vesicles were loaded onto gels based on protein concentration (50–100 μg of protein). Viral lysates were loaded based on volume of viral supernatant (0.5–2.5 mL). Proteins was resolved on 10–15% SDS–polyacrylamide gel electrophoresis and electro transferred onto a nitrocellulose membrane, probed using antibodies against Myomaker (1:500, provided from Dr. Leonid Chernomordik laboratory; custom generated by YenZym; epitope is 110–160 amino acid sequence of human TMEM8C), Myomerger (1:1000, #AF4580, R&D), VSV-G (1:1000, #8G5F11, Kerafast), V5 (1:1000, #R96025,

Invitrogen), VSV-M (1:1000, #23H12, Kerafast), VSV-N (1:000, #10G4, Kerafast), HIV-Gag (p55, p24, p17; 1:1000, #ab63917, Abcam) and GAPDH (1:2000, #MAB374, Millipore) followed by secondary antibodies against rabbit, sheep, or mouse conjugated to Alexa-Fluor 680 (Invitrogen), DyLight 680, or DyLight 800 (Cell Signaling Technology). Bands were visualized using the Odyssey infrared detection system (LI-COR Biosciences).

For μDystrophin detection in muscle lysates by western blot, flash-frozen muscle samples were pulverized in liquid nitrogen and the tissue powder immediately suspended in pre-chilled lysis buffer [20 mM Tris, 0.5 mM EdTA, 0.5% Triton X-100, pH 7.4, containing 1X protease inhibitor cocktail (# 78437, Thermo Scientific), 1X phosphatase inhibitor cocktail (#P5726, Sigma), 1mM DTT, and 10 mM sodium fluoride]. Samples were manually homogenized (40–50 strokes) on ice using a frosted Kontes Duall all glass tissue grinder (#885450–0020, DWK Life Sciences). Solubilization was then allowed to proceed by incubating homogenized samples on a rotator for 90 minutes at 4°C before determining protein concentration using a Bradford protein assay kit (#5000006, BioRad). Samples were prepped in 1X Laemmli buffer (containing 100 mM DTT) at 1 μg/mL and stored at −20°C. Samples were then denatured by heating (75 °C for 25 minutes and then at 95°C for 5 minutes) immediately before being resolved on a discontinuous reducing 4.5% polyacrylamide gel and subsequently transferred to PVDF membranes (2-hour transfer at 400mA/~56V/~23W in methanol-free ice-cold transfer buffer (48mM Tris, 39mM Glycine, pH 8.6 + 0.037% SDS) with constant stirring in 4°C cold-room). Membranes were then washed 3 times in 1X TBST for 5 minutes each before being blocked in 5% non-fat dry-milk in 1X TBST for 45-minutes at room temperature. Membranes were then probed against dystrophin (1:400, #MANEX1011B(1C7), DSHB) in 5% BSA in 1X TBST overnight at 4°C and subsequently in secondary anti-mouse 680 IRDye antibody [1:5000, #926–68072, Licor) for 1 hour before being imaged on Odyssey Licor Imaging system.

Metric for quantification of restoration of μDys expression is percentage of full-length dystrophin expression in wild-type muscle, and was calculated as previously described[59], using regression analysis of a 5-point standard curve constructed by immunoblotting increasing dilutions of wild-type (100%, 50%, 25%, and 12.5%) and 100% of dystrophic (negative for dystrophin) protein samples processed as described above.

Transmission electron microscopy—Lentiviral particles were placed on a Formvar Carbon Film (400 mesh, copper, Electron Microscopy Sciences) and processed for electron microscopy by staining with 1% ammonium molybdate. Viral particles were examined under a H-7650 Transmission Electron Microscope (Hitachi) at 80 kV.

Immunogold electron microscopy—For detection of Myomaker, Myomerger, and VSV-G on lentiviral particles, virions purified by ultracentrifugation and a sucrose cushion were placed on a Formvar Carbon Film as described above, followed by blocking with 1% BSA for one hour and incubation in primary antibodies targeting Myomaker (1:10, # SC-244459, Santa Cruz), Myomerger (1:20, #AF4580, R&D), or VSV-G (1:20, #8G5F11, Kerafast) in 1% BSA overnight at 4°C followed by gold-conjugated secondary antibodies against goat (12 nm, 1:20, #705-205-147, Jackson ImmunoResearch), sheep (6 nm, 1:20, #713-195-147, Jackson ImmunoResearch) or mouse (12 nm, 1:20, # 715-205-150, Jackson

ImmunoResearch) respectively. Finally samples were negatively stained with 2% PTA for 5 minute, after which samples were blotted on a drop of water and left to dry for 5 minutes at room temperatures. Labeled viral particles were then examined under a H-7650 Transmission Electron Microscope (Hitachi) at 80 kV.

Muscle histology—For tdTomato analysis, skeletal and non-skeletal muscle tissues were isolated and fixed in 2% PFA/PBS overnight at 4°C then placed in 20% sucrose/PBS at 4°C for at least 4 hours. Tissues were embedded in optimal cutting temperature (OCT) compound (Sakura Finetek, Torrance, CA, USA) and frozen, then 10 μm sections were collected. The sections were mounted with VectaShield containing DAPI (Vector Laboratories, Burlingame, CA, USA).

For analysis of μDystrophin expression by immunohistochemistry, muscle tissues were coated with talcum powder and snap frozen in liquid nitrogen. Tissues were then embedded in OCT compound and 10-μm sections were collected. For experiments in Figures 2H, 4B, S5B, S5C, S5D, 6B, sections were fixed in ice-cold acetone for 10 minutes, blocked with 2% BSA/PBS for 30 minutes and incubated with anti-Dystrophin (Dy10/12B2) (1:50, #GTX01869, GeneTex) followed by secondary antibody Alexa Fluor 546 (#A-11018, Invitrogen). For experiments in Figures S6A and S6E, muscle sections were directly blocked with 2% BSA (without prior fixation) followed by incubation with anti-Dystrophin (Dy10/12B2) (1:50, #GTX01869, GeneTex) as described above followed by secondary antibody Alexa Fluor 568 (#A-21134, Invitrogen) or Alexa Fluor 488 (#A-21131, Invitrogen). Along with dystrophin antibodies, some sections were incubated with anti-Laminin antibody (#L9393, Sigma Aldrich) followed by secondary antibody Alexa Fluor 555 (#A-31572, Invitrogen) or Alexa Fluor 488 (#A-21206, Invitrogen). All antibodies were diluted in blocking solution and incubated on sections overnight at 4°C. All sections were mounted with VectaShield containing DAPI. All immunostaining in vitro and in vivo was visualized with a Nikon Eclipse Ti inverted microscope with A1R confocal running NIS Elements (Nikon, Tokyo, Japan), and images were analyzed with Fiji (ImageJ, National Institutes of Health, Bethesda, MD, USA).

Masson's Trichrome staining was performed for analysis of fibrosis in diaphragm muscles using a commercially available kit. 10 μm sections were prepared from frozen diaphragm muscles and were stained following a protocol suggested by the manufacturer (Richard-Allan Scientific).

Muscle function and membrane integrity analysis—*Mdx*^{4cv} mice treated with 3x RO injections of Bald- or Mymk+Mymg-LV-μDys were subjected to functional analysis 6 months after the last injection. Muscle performance was measured *in vivo* with a 300C-LRmuscle lever system (Aurora Scientific Inc., Aurora, CAN), as previously described[60]. Nerve evoked muscle function in vivo was in animals anesthetized via inhalation (~3% isoflurane, SomnoSuite, Kent Scientific), and placed on a thermostatically controlled table with anesthesia maintained via nose-cone (~2% isoflurane). The knee position was fixed and the foot firmly fixed to the footplate on the motor shaft. Contraction of the plantarflexors were elicited by percutaneous electrical stimulation of the tibial nerve at a current for optimal isometric twitch torque (0.2 msec). The force vs stimulation frequency relationship

was determined by a series of pulse trains (500 msec) at increasing frequency: 1, 20, 40, 50, 60, 80, 100 and 150 Hz. Following assessment of the isometric torque vs frequency, the susceptibility to contraction injury was assayed with 20 eccentric contractions as previously described at maximal isometric torque (150 ms duration, 0.2-ms pulse train at 150 Hz). Eccentric contractions were achieved by translating the footplate 40° backward at a velocity of 800°/s after the first 100 ms of the isometric contraction. The decrease in the peak isometric force before the eccentric phase was taken as an indication of muscle damage.

Diaphragmatic function was assessed ex vivo using methods previously described[61]. From the diaphragm removed en bloc and a strip was dissected, affixed with microclips to the rib and central tendon, and mounted in an in vitro bath between a fixed post and force transducer (300C-LR; Aurora Scientific) operated in isometric mode. Muscles were maintained in physiological saline solution (pH 7.6) containing (in mM) 119 NaCl, 5 KCl, 1 $MgSO_4$, 5 $NaHCO_3$, 1.25 $CaCl_2$, 1 KH_2PO_4, 10 HEPES, and 10 glucose and maintained at 30°C under aeration with 95% O_2 and 5% CO_2 throughout the experiment. Resting tension was iteratively adjusted for each muscle to obtain optimal twitch force. During a 5-minute equilibration period, single twitches were elicited at every 30 seconds with electrical pulses (0.2 ms) via platinum electrodes running parallel to the muscle. Optimal resting tension was determined, and isometric tension was evaluated by 250 ms trains of pulses delivered at 1, 20, 40, 50, 60, 80, 100, 150, and 300 Hz.

To assess muscle fiber membrane stability following treatment with Bald- or Mymk+Mymg-LV-μDys, mice were injected intraperitoneally with Evan's blue dye (EBD) (#E2129–10G, Sigma) (10 mg/mL in sterile PBS at a dose of 0.1 mL/10 g mouse body weight). One gastrocnemius muscle was subjected to eccentric contraction after 24 hours and all muscle groups were harvested 24 hours later. 10 μm sections were then prepared from frozen gastrocnemius and diaphragm muscles followed by staining with laminin (as described above) and EBD^+ fibers were visualized using the 647nm laser of a Nikon Eclipse Ti inverted microscope with A1R confocal running NIS Elements (Nikon, Tokyo, Japan), and images were analyzed with Fiji (ImageJ, National Institutes of Health, Bethesda, MD, USA).

Bioluminescence imaging—Mice were injected with 150 mg/kg of D-luciferin (Promega, Cat. # E1605 or Goldbio, Cat. # LUCK-2G) and anesthetized with isoflurane before imaging. The bioluminescence images were acquired 7 min after D-luciferin injection with a rate of one image per 1 minute for 30 minutes using the IVIS spectrum CT in vivo imaging system (PerkinElmer, Cat#128201). Total radiance was measured from the same size of the region of interest (ROI) using Living Image 4.7.3 software (PerkinElmer). The highest captured radiance over imaging time was determined as the peak of the kinetic curve and chosen for analysis.

FACS analysis—For analysis of pseudotyped lentiviral transduction in mononuclear myogenic cells in vivo, tibialis anterior muscles were harvested and subjected to enzymatic digestion by collagenase and pronase. Mononuclear cell suspensions were incubated with antibodies against α7-integrin (MBL International, Woburn, MA, USA) and Alexa Fluor 488 for detection of myogenic cells and CD45, CD31, Sca1 and Ter119 for negative selection (all Alexa Fluor 700 conjugated, eBiosciences). FACS analysis was performed

on a FACSCanto (BD Biosciences) or LSRFortessa (BD Biosciences). Contour plots of data were generated with FlowJo v10.8.1 software.

Quantification and statistical analysis—Quantification was combined from at least two independent experiments, each with technical replicates. At least two independent viral or EV preparations were utilized and these preps were produced from at least two independent cell lines. Sample sizes and replicates for each experiment are noted in the figure legends. Data were processed and analyzed using Microsoft Excel and GraphPad Prism 9 software. In all graphs, error bars indicate the standard deviation (SD). Data were compared between groups using various statistical tests based on number of groups, normality of data, variance of standard deviations, and multiple comparisons. Specific statistical tests are noted in the figure legends. The criterion for statistical significance was *p< 0.05, **p< 0.01, ***p< 0.001, ****p< 0.0001.

Supplementary Material

Refer to Web version on PubMed Central for supplementary material.

Acknowledgments

We thank members of the Millay laboratory and N. Scott Blair (Molkentin lab) for reagents and discussion; Dr. Niclas E Bengtsson (University of Washington) for advice and technical assistance; Victoria Summey of the Cincinnati Children's Hospital Medical Center Comprehensive Mouse and Cancer Core for help with retro-orbital injections; Thouwa Samake and Phoebe Franz of the Cincinnati Children's Hospital Medical Center Viral Vector Core for their help with lentiviral purification. This work was mainly supported by a grant to D.P.M. from the National Institutes of Health (R61AR076771). Work in the Millay laboratory is also funded by grants to D.P.M. from Children's Hospital Research Foundation, National Institutes of Health (R01AR068286, R01AG059605), and a sponsored research agreement with Sana Biotechnology. Work in the Podbilewicz laboratory is funded by grants to B.P. from the Israel Science Foundation (grants 257/17, 2462/18, 2327/19, and 178/20). The Chamberlain laboratory is supported by the Sen. Paul D. Wellstone Muscular Dystrophy Specialized Research Center (P50 AR065139).

References

1. Martens S & McMahon HT Mechanisms of membrane fusion: disparate players and common principles. Nat Rev Mol Cell Biol 9, 543–556, doi:10.1038/nrm2417 (2008). [PubMed: 18496517]
2. Brukman NG, Uygur B, Podbilewicz B & Chernomordik LV How cells fuse. J Cell Biol 218, 1436–1451, doi:10.1083/jcb.201901017 (2019). [PubMed: 30936162]
3. Segev N, Avinoam O & Podbilewicz B Fusogens. Curr Biol 28, R378–R380, doi:10.1016/j.cub.2018.01.024 (2018). [PubMed: 29689218]
4. Milone MC & O'Doherty U Clinical use of lentiviral vectors. Leukemia 32, 1529–1541, doi:10.1038/s41375-018-0106-0 (2018). [PubMed: 29654266]
5. Cronin J, Zhang XY & Reiser J Altering the tropism of lentiviral vectors through pseudotyping. Curr Gene Ther 5, 387–398, doi:10.2174/1566523054546224 (2005). [PubMed: 16101513]
6. Nie J, Li Q, Wu J, Zhao C, Hao H, Liu H, Zhang L, Nie L, Qin H, Wang M, Lu Q, Li X, Sun Q, Liu J, Fan C, Huang W, Xu M & Wang Y Quantification of SARS-CoV-2 neutralizing antibody by a pseudotyped virus-based assay. Nat Protoc 15, 3699–3715, doi:10.1038/s41596-020-0394-5 (2020). [PubMed: 32978602]
7. Avinoam O, Fridman K, Valansi C, Abutbul I, Zeev-Ben-Mordehai T, Maurer UE, Sapir A, Danino D, Grunewald K, White JM & Podbilewicz B Conserved eukaryotic fusogens can fuse viral envelopes to cells. Science 332, 589–592, doi:10.1126/science.1202333 (2011). [PubMed: 21436398]

8. Valansi C, Moi D, Leikina E, Matveev E, Grana M, Chernomordik LV, Romero H, Aguilar PS & Podbilewicz B Arabidopsis HAP2/GCS1 is a gamete fusion protein homologous to somatic and viral fusogens. J Cell Biol 216, 571–581, doi:10.1083/jcb.201610093 (2017). [PubMed: 28137780]
9. Bi P, Ramirez-Martinez A, Li H, Cannavino J, McAnally JR, Shelton JM, Sanchez-Ortiz E, Bassel-Duby R & Olson EN Control of muscle formation by the fusogenic micropeptide myomixer. Science 356, 323–327, doi:10.1126/science.aam9361 (2017). [PubMed: 28386024]
10. Millay DP, O'Rourke JR, Sutherland LB, Bezprozvannaya S, Shelton JM, Bassel-Duby R & Olson EN Myomaker is a membrane activator of myoblast fusion and muscle formation. Nature 499, 301–305, doi:10.1038/nature12343 (2013). [PubMed: 23868259]
11. Quinn ME, Goh Q, Kurosaka M, Gamage DG, Petrany MJ, Prasad V & Millay DP Myomerger induces fusion of non-fusogenic cells and is required for skeletal muscle development. Nat Commun 8, 15665, doi:10.1038/ncomms15665 (2017). [PubMed: 28569755]
12. Zhang Q, Vashisht AA, O'Rourke J, Corbel SY, Moran R, Romero A, Miraglia L, Zhang J, Durrant E, Schmedt C, Sampath SC & Sampath SC The microprotein Minion controls cell fusion and muscle formation. Nat Commun 8, 15664, doi:10.1038/ncomms15664 (2017). [PubMed: 28569745]
13. Millay DP Regulation of the myoblast fusion reaction for muscle development, regeneration, and adaptations. Exp Cell Res 415, 113134, doi:10.1016/j.yexcr.2022.113134 (2022). [PubMed: 35367215]
14. Duncan R Fusogenic Reoviruses and Their Fusion-Associated Small Transmembrane (FAST) Proteins. Annu Rev Virol 6, 341–363, doi:10.1146/annurev-virology-092818-015523 (2019). [PubMed: 31283438]
15. Leikina E, Gamage DG, Prasad V, Goykhberg J, Crowe M, Diao J, Kozlov MM, Chernomordik LV & Millay DP Myomaker and Myomerger Work Independently to Control Distinct Steps of Membrane Remodeling during Myoblast Fusion. Dev Cell 46, 767–780 e767, doi:10.1016/j.devcel.2018.08.006 (2018). [PubMed: 30197239]
16. Kim JH & Chen EH The fusogenic synapse at a glance. J Cell Sci 132, doi:10.1242/jcs.213124 (2019).
17. Duan D, Goemans N, Takeda S, Mercuri E & Aartsma-Rus A Duchenne muscular dystrophy. Nat Rev Dis Primers 7, 13, doi:10.1038/s41572-021-00248-3 (2021). [PubMed: 33602943]
18. Tabebordbar M, Lagerborg KA, Stanton A, King EM, Ye S, Tellez L, Krunnfusz A, Tavakoli S, Widrick JJ, Messemer KA, Troiano EC, Moghadaszadeh B, Peacker BL, Leacock KA, Horwitz N, Beggs AH, Wagers AJ & Sabeti PC Directed evolution of a family of AAV capsid variants enabling potent muscle-directed gene delivery across species. Cell 184, 4919–4938 e4922, doi:10.1016/j.cell.2021.08.028 (2021). [PubMed: 34506722]
19. Crudele JM & Chamberlain JS AAV-based gene therapies for the muscular dystrophies. Hum Mol Genet 28, R102–R107, doi:10.1093/hmg/ddz128 (2019). [PubMed: 31238336]
20. Bulcha JT, Wang Y, Ma H, Tai PWL & Gao G Viral vector platforms within the gene therapy landscape. Signal Transduct Target Ther 6, 53, doi:10.1038/s41392-021-00487-6 (2021). [PubMed: 33558455]
21. Gregory LG, Waddington SN, Holder MV, Mitrophanous KA, Buckley SM, Mosley KL, Bigger BW, Ellard FM, Walmsley LE, Lawrence L, Al-Allaf F, Kingsman S, Coutelle C & Themis M Highly efficient EIAV-mediated in utero gene transfer and expression in the major muscle groups affected by Duchenne muscular dystrophy. Gene Ther 11, 1117–1125, doi:10.1038/sj.gt.3302268 (2004). [PubMed: 15141156]
22. Kimura E, Li S, Gregorevic P, Fall BM & Chamberlain JS Dystrophin delivery to muscles of mdx mice using lentiviral vectors leads to myogenic progenitor targeting and stable gene expression. Mol Ther 18, 206–213, doi:10.1038/mt.2009.253 (2010). [PubMed: 19888194]
23. Kobinger GP, Louboutin JP, Barton ER, Sweeney HL & Wilson JM Correction of the dystrophic phenotype by in vivo targeting of muscle progenitor cells. Hum Gene Ther 14, 1441–1449, doi:10.1089/104303403769211655 (2003). [PubMed: 14577924]
24. Li S, Kimura E, Fall BM, Reyes M, Angello JC, Welikson R, Hauschka SD & Chamberlain JS Stable transduction of myogenic cells with lentiviral vectors expressing a minidystrophin. Gene Ther 12, 1099–1108, doi:10.1038/sj.gt.3302505 (2005). [PubMed: 15759015]

25. MacKenzie TC, Kobinger GP, Louboutin JP, Radu A, Javazon EH, Sena-Esteves M, Wilson JM & Flake AW Transduction of satellite cells after prenatal intramuscular administration of lentiviral vectors. J Gene Med 7, 50–58, doi:10.1002/jgm.649 (2005). [PubMed: 15515139]
26. Whitt MA Generation of VSV pseudotypes using recombinant DeltaG-VSV for studies on virus entry, identification of entry inhibitors, and immune responses to vaccines. J Virol Methods 169, 365–374, doi:10.1016/j.jviromet.2010.08.006 (2010). [PubMed: 20709108]
27. Meledin A, Li X, Matveev E, Gildor B, Katzir O & Podbilewicz B EFF-1 promotes muscle fusion, paralysis and retargets infection by AFF-1-coated viruses in C. elegans. bioRxiv, 2020.2005.2017.099622, doi:10.1101/2020.05.17.099622 (2020).
28. Kopecky SA, Willingham MC & Lyles DS Matrix protein and another viral component contribute to induction of apoptosis in cells infected with vesicular stomatitis virus. J Virol 75, 12169–12181, doi:10.1128/JVI.75.24.12169-12181.2001 (2001). [PubMed: 11711608]
29. van Niel G, D'Angelo G & Raposo G Shedding light on the cell biology of extracellular vesicles. Nat Rev Mol Cell Biol 19, 213–228, doi:10.1038/nrm.2017.125 (2018). [PubMed: 29339798]
30. Herrmann IK, Wood MJA & Fuhrmann G Extracellular vesicles as a next-generation drug delivery platform. Nat Nanotechnol 16, 748–759, doi:10.1038/s41565-021-00931-2 (2021). [PubMed: 34211166]
31. Goh Q & Millay DP Requirement of myomaker-mediated stem cell fusion for skeletal muscle hypertrophy. Elife 6, doi:10.7554/eLife.20007 (2017).
32. O'Brien KF & Kunkel LM Dystrophin and muscular dystrophy: past, present, and future. Mol Genet Metab 74, 75–88, doi:10.1006/mgme.2001.3220 (2001). [PubMed: 11592805]
33. Ramos JN, Hollinger K, Bengtsson NE, Allen JM, Hauschka SD & Chamberlain JS Development of Novel Micro-dystrophins with Enhanced Functionality. Mol Ther 27, 623–635, doi:10.1016/j.ymthe.2019.01.002 (2019). [PubMed: 30718090]
34. Maesner CC, Almada AE & Wagers AJ Established cell surface markers efficiently isolate highly overlapping populations of skeletal muscle satellite cells by fluorescence-activated cell sorting. Skelet Muscle 6, 35, doi:10.1186/s13395-016-0106-6 (2016). [PubMed: 27826411]
35. Zhang H, Wen J, Bigot A, Chen J, Shang R, Mouly V & Bi P Human myotube formation is determined by MyoD-Myomixer/Myomaker axis. Sci Adv 6, doi:10.1126/sciadv.abc4062 (2020).
36. McGeachie JK, Grounds MD, Partridge TA & Morgan JE Age-related changes in replication of myogenic cells in mdx mice: quantitative autoradiographic studies. J Neurol Sci 119, 169–179, doi:10.1016/0022-510x(93)90130-q (1993). [PubMed: 8277331]
37. Petrany MJ, Song T, Sadayappan S & Millay DP Myocyte-derived Myomaker expression is required for regenerative fusion but exacerbates membrane instability in dystrophic myofibers. JCI Insight 5, doi:10.1172/jci.insight.136095 (2020).
38. Kishimoto TK & Samulski RJ Addressing high dose AAV toxicity - 'one and done' or 'slower and lower'? Expert Opin Biol Ther 22, 1067–1071, doi:10.1080/14712598.2022.2060737 (2022). [PubMed: 35373689]
39. Wahlgren L, Kroksmark AK, Tulinius M & Sofou K One in five patients with Duchenne muscular dystrophy dies from other causes than cardiac or respiratory failure. Eur J Epidemiol 37, 147–156, doi:10.1007/s10654-021-00819-4 (2022). [PubMed: 34802091]
40. Connolly JB Lentiviruses in gene therapy clinical research. Gene Ther 9, 1730–1734, doi:10.1038/sj.gt.3301893 (2002). [PubMed: 12457288]
41. Escors D & Breckpot K Lentiviral vectors in gene therapy: their current status and future potential. Arch Immunol Ther Exp (Warsz) 58, 107–119, doi:10.1007/s00005-010-0063-4 (2010). [PubMed: 20143172]
42. DePolo NJ, Reed JD, Sheridan PL, Townsend K, Sauter SL, Jolly DJ & Dubensky TW Jr. VSV-G pseudotyped lentiviral vector particles produced in human cells are inactivated by human serum. Mol Ther 2, 218–222, doi:10.1006/mthe.2000.0116 (2000). [PubMed: 10985952]
43. Themis M, Waddington SN, Schmidt M, von Kalle C, Wang Y, Al-Allaf F, Gregory LG, Nivsarkar M, Themis M, Holder MV, Buckley SM, Dighe N, Ruthe AT, Mistry A, Bigger B, Rahim A, Nguyen TH, Trono D, Thrasher AJ & Coutelle C Oncogenesis following delivery of a nonprimate lentiviral gene therapy vector to fetal and neonatal mice. Mol Ther 12, 763–771, doi:10.1016/j.ymthe.2005.07.358 (2005). [PubMed: 16084128]

44. Schlimgen R, Howard J, Wooley D, Thompson M, Baden LR, Yang OO, Christiani DC, Mostoslavsky G, Diamond DV, Duane EG, Byers K, Winters T, Gelfand JA, Fujimoto G, Hudson TW & Vyas JM Risks Associated With Lentiviral Vector Exposures and Prevention Strategies. J Occup Environ Med 58, 1159–1166, doi:10.1097/JOM.0000000000000879 (2016). [PubMed: 27930472]
45. Cai Y, Laustsen A, Zhou Y, Sun C, Anderson MV, Li S, Uldbjerg N, Luo Y, Jakobsen MR & Mikkelsen JG Targeted, homology-driven gene insertion in stem cells by ZFN-loaded 'all-in-one' lentiviral vectors. Elife 5, doi:10.7554/eLife.12213 (2016).
46. Duan D Systemic AAV Micro-dystrophin Gene Therapy for Duchenne Muscular Dystrophy. Mol Ther 26, 2337–2356, doi:10.1016/j.ymthe.2018.07.011 (2018). [PubMed: 30093306]
47. Morales L, Gambhir Y, Bennett J & Stedman HH Broader Implications of Progressive Liver Dysfunction and Lethal Sepsis in Two Boys following Systemic High-Dose AAV. Mol Ther 28, 1753–1755, doi:10.1016/j.ymthe.2020.07.009 (2020). [PubMed: 32710826]
48. Morgan J & Muntoni F Changes in Myonuclear Number During Postnatal Growth - Implications for AAV Gene Therapy for Muscular Dystrophy. J Neuromuscul Dis 8, S317–S324, doi:10.3233/JND-210683 (2021). [PubMed: 34334413]
49. Manini A, Abati E, Nuredini A, Corti S & Comi GP Adeno-Associated Virus (AAV)-Mediated Gene Therapy for Duchenne Muscular Dystrophy: The Issue of Transgene Persistence. Front Neurol 12, 814174, doi:10.3389/fneur.2021.814174 (2021). [PubMed: 35095747]
50. Pawlikowski B, Pulliam C, Betta ND, Kardon G & Olwin BB Pervasive satellite cell contribution to uninjured adult muscle fibers. Skelet Muscle 5, 42, doi:10.1186/s13395-015-0067-1 (2015). [PubMed: 26668715]
51. Cutler AA, Pawlikowski B, Wheeler JR, Dalla Betta N, Elston T, O'Rourke R, Jones K & Olwin BB The regenerating skeletal muscle niche drives satellite cell return to quiescence. iScience 25, 104444, doi:10.1016/j.isci.2022.104444 (2022). [PubMed: 35733848]
52. Duverge A & Negroni M Pseudotyping Lentiviral Vectors: When the Clothes Make the Virus. Viruses 12, doi:10.3390/v12111311 (2020).
53. Milani M, Annoni A, Moalli F, Liu T, Cesana D, Calabria A, Bartolaccini S, Biffi M, Russo F, Visigalli I, Raimondi A, Patarroyo-White S, Drager D, Cristofori P, Ayuso E, Montini E, Peters R, Iannacone M, Cantore A & Naldini L Phagocytosis-shielded lentiviral vectors improve liver gene therapy in nonhuman primates. Sci Transl Med 11, doi:10.1126/scitranslmed.aav7325 (2019).
54. Kaariainen L & Gomatos PJ A kinetic analysis of the synthesis in BHK 21 cells of RNAs specific for Semliki Forest virus. J Gen Virol 5, 251–265, doi:10.1099/0022-1317-5-2-251 (1969). [PubMed: 5388361]
55. Mitani Y, Vagnozzi RJ & Millay DP In vivo myomaker-mediated heterologous fusion and nuclear reprogramming. FASEB J 31, 400–411, doi:10.1096/fj.201600945R (2017). [PubMed: 27825107]
56. Yang X, Boehm JS, Yang X, Salehi-Ashtiani K, Hao T, Shen Y, Lubonja R, Thomas SR, Alkan O, Bhimdi T, Green TM, Johannessen CM, Silver SJ, Nguyen C, Murray RR, Hieronymus H, Balcha D, Fan C, Lin C, Ghamsari L, Vidal M, Hahn WC, Hill DE & Root DE A public genome-scale lentiviral expression library of human ORFs. Nat Methods 8, 659–661, doi:10.1038/nmeth.1638 (2011). [PubMed: 21706014]
57. Millay DP, Sutherland LB, Bassel-Duby R & Olson EN Myomaker is essential for muscle regeneration. Genes Dev 28, 1641–1646, doi:10.1101/gad.247205.114 (2014). [PubMed: 25085416]
58. Hindi SM, Shin J, Gallot YS, Straughn AR, Simionescu-Bankston A, Hindi L, Xiong G, Friedland RP & Kumar A MyD88 promotes myoblast fusion in a cell-autonomous manner. Nat Commun 8, 1624, doi:10.1038/s41467-017-01866-w (2017). [PubMed: 29158520]
59. Birch SM, Lawlor MW, Conlon TJ, Guo LJ, Crudele JM, Hawkins EC, Nghiem PP, Ahn M, Meng H, Beatka MJ, Fickau BA, Prieto JC, Styner MA, Struharik MJ, Shanks C, Brown KJ, Golebiowski D, Bettis AK, Balog-Alvarez CJ, Clement N, Coleman KE, Corti M, Pan X, Hauschka SD, Gonzalez JP, Morris CA, Schneider JS, Duan D, Chamberlain JS, Byrne BJ & Kornegay JN Assessment of systemic AAV-microdystrophin gene therapy in the GRMD model of Duchenne muscular dystrophy. Sci Transl Med 15, eabo1815, doi:10.1126/scitranslmed.abo1815 (2023). [PubMed: 36599002]

60. Boyer JG, Huo J, Han S, Havens JR, Prasad V, Lin BL, Kass DA, Song T, Sadayappan S, Khairallah RJ, Ward CW & Molkentin JD Depletion of skeletal muscle satellite cells attenuates pathology in muscular dystrophy. Nat Commun 13, 2940, doi:10.1038/s41467-022-30619-7 (2022). [PubMed: 35618700]

61. Geist Hauserman J, Stavusis J, Joca HC, Robinett JC, Hanft L, Vandermeulen J, Zhao R, Stains JP, Konstantopoulos K, McDonald KS, Ward C & Kontrogianni-Konstantopoulos A Sarcomeric deficits underlie MYBPC1-associated myopathy with myogenic tremor. JCI Insight 6, doi:10.1172/jci.insight.147612 (2021).

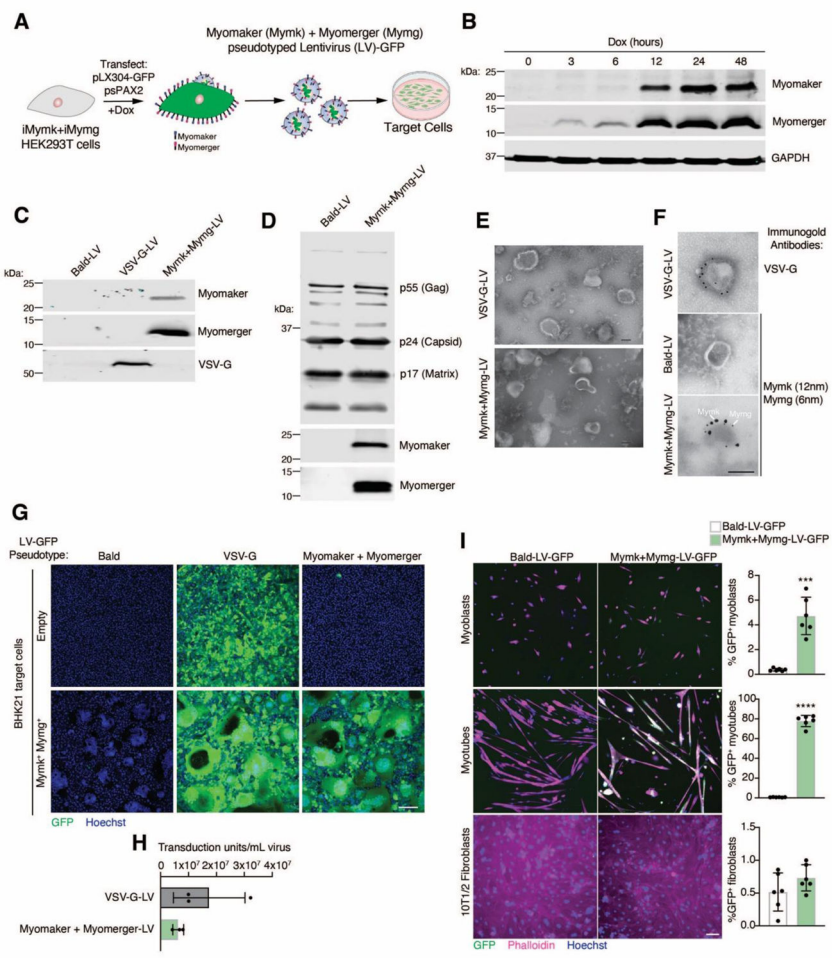

Figure 1. Engineering and characterization of lentiviruses pseudotyped with Myomaker and Myomerger.

(A) Schematic showing production of lentiviruses (LV) from Myomaker- and Myomerger-expressing HEK293T cells.

(B) Western blot for Myomaker, Myomerger, and GAPDH on HEK293T cell lysates after various times of doxycycline treatment.

(C) Western blot on concentrated viral particles for Myomaker, Myomaker, and VSV-G.

(D) Western blot on Bald-LVs and Mymk+Mymg-LVs for viral components and the muscle fusogens.

(E) Representative images from transmission electron microscopy on VSV-G-LVs and Mymk+Mymg-LVs. Scale bar, 100 nm.

(F) Images from immunogold electron microscopy using the indicated antibodies on the pseudotyped lentiviruses. Myomaker and Myomerger antibodies were detected in the same sample using gold particles of different sizes. Scale bar, 200 nm.

(G) Representative images of empty and Mymk+Mymg target cells after application of Bald GFP-encoding LVs or LVs pseudotyped with VSV-G or Myomaker and Myomerger. Nuclei were stained with Hoechst. Scale bar, 100 μm.

(H) Quantification of titers for VSV-G-LVs and Mymk+Mymk-LVs prior to concentration of supernatants. Each sample is an average of 3–4 replicates from independent viral preparations. Titers were determined on Mymk+Mymg BHK21 cells.
(I) Representative images from cultures of differentiated myotubes, proliferating myoblasts, and fibroblasts that were treated with Bald-LV-GFP or Mymk+Mymg-LV-GFP. Cells were stained with Phalloidin and Hoechst. Scale bar, 100 μm. GFP^+ cells were quantified for each cell type and histograms are shown on the right.
Data are presented as mean ± standard deviation. Statistical test used was an unpaired t-test with Welch's correction; ***p<0.001, ****p<0.0001.

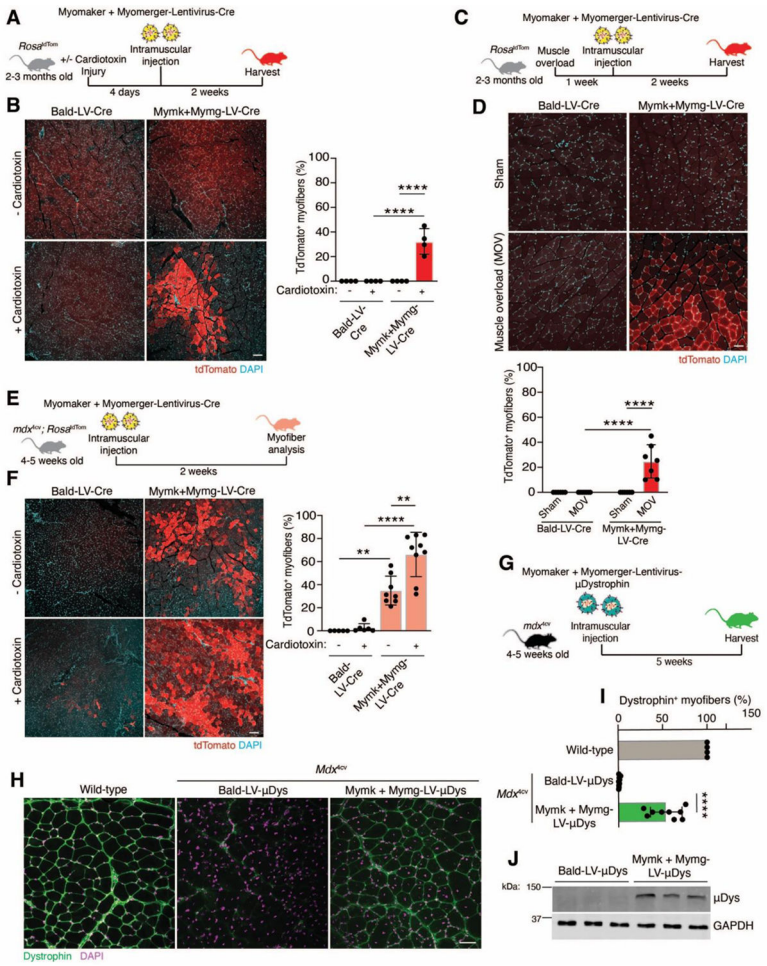

Figure 2. Mymk+Mymg-LVs transduce activated skeletal muscle in vivo.

(A) Lentiviruses encoding for Cre recombinase and pseudotyped with Myomaker and Myomerger (Mymk+Mymg-LV-Cre) were produced and delivered to the tibialis anterior muscles of *Rosa*^{tdTom} mice through direct intramuscular injection. Some tibialis anterior muscles were injured with cardiotoxin prior to receiving lentivirus.

(B) Representative images are shown displaying tdTomato^{+} myofibers after injury and regeneration. Nuclei were stained with DAPI. The percentage of tdTomato^{+} myofibers is shown (right panel). Scale bar, 100 µm.

(C) Similar setup as in (A) except muscle overload, which causes hypertrophy, was performed and lentiviruses were injected into the plantaris.

(D) Representative images are shown for sham and overloaded muscles treated intramuscularly with Bald-LV-Cre or Mymk+Mymg-LV-Cre. Nuclei were stained with DAPI. Scale bar, 50 µm. Quantification of the percentage of tdTomato^{+} myofibers (bottom panel).

(E) *Mdx*^{4cv}; *Rosa*^{tdTom} mice were used as recipients for Bald-LV-Cre or Mymk+Mymg-LV-Cre. Tibialis anterior muscles receiving lentiviruses through intramuscular injection were uninjured or previously injured with cardiotoxin.

(F) Representative images showing tdTomato$^+$ myofibers with and without cardiotoxin injury. Nuclei were stained with DAPI. Scale bar, 100 μm. Quantification of the percentage of tdTomato$^+$ myofibers (right panel).
(G) Schematic for experimental plan to assess transduction of Myomaker and Myomerger-pseudotyped lentiviruses packaged with μDystrophin (μDys) after intramuscular injection.
(H) Immunostaining for dystrophin from tibialis anterior muscles from wild-type or *mdx*^{4cv} mice that were injected with Bald- or Myomaker and Myomerger-lentiviruses encoding μDys. Nuclei were stained with DAPI. Scale bar, 100 μm.
(I) Quantification of the percentage of μDys$^+$ myofibers from (H).
(J) Western blot for μDys from tibialis anterior muscle lysates after injection of Bald-LV-μDys or Mymk+Mymg-LV-μDys.
Data are presented as mean ± standard deviation and combined from at least two independent lentiviral preparations.
Statistical tests used were (B, D, F) Two-way ANOVA with Tukey's correction for multiple comparisons; (I) One-way ANOVA with Tukey's correction for multiple comparisons; **p< 0.01, ****p< 0.0001.

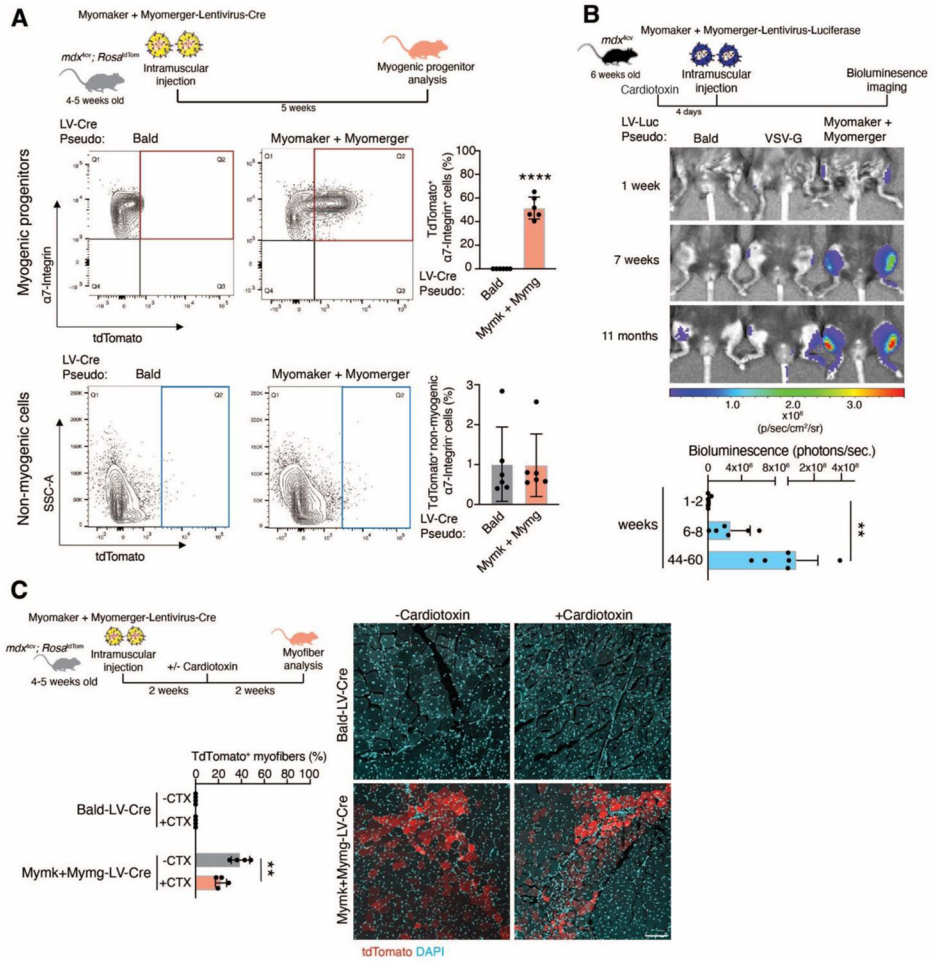

Figure 3. Myogenic progenitors in dystrophic mice are transduced by lentiviruses pseudotyped with Myomaker and Myomerger.

(A) Top panel displays experimental design for analysis of muscle progenitors. Middle panels show representative FACS plots and quantification for α7-Integrin^{+} myogenic cells (y-axis) and tdTomato^{+} cells (x-axis) from *mdx*^{4cv}; *Rosa*^{tdTom} muscle that received Bald-LV-Cre or Mymk+Mymg-LV-Cre. Bottom panels show representative FACS plots and quantification for tdTomato^{+} non-myogenic interstitial cells.

(B) Top panel is the experimental design using lentivirus encoding for luciferase that was pseudotyped with Bald, VSV-G, or Myomaker and Myomerger. After cardiotoxin injury, lentiviruses were injected intramuscularly and bioluminesence measured through IVIS imaging multiple time points after viral delivery. Representative pseudocolored images show a progressive increase in bioluminescence in the muscles treated with Myomaker and Myomerger-pseudotyped virus. Bottom panel is quantification of bioluminescence for muscles transduced with lentivirus containing Myomaker and Myomerger.

(C) *Mdx*^{4cv}; *Rosa*^{tdTom} mice received an intramuscular injection of Bald-LV-Cre or Mymk+Mymg-LV-Cre, then 2 weeks later some mice were injured with cardiotoxin. Representative images for tdTomato^{+} myofibers are shown to the right. Nuclei were stained with DAPI. Scale bar, 100 μm. Bottom, left panel shows quantification of the percentage of tdTomato^{+} myofibers.

Data are presented as mean ± standard deviation; data in (A, B) combined from at least two independent lentiviral preparations; data in (C) is from one lentiviral preparation. Statistical tests used were (A) unpaired t-test with Welch's correction; (B) Friedman test with Dunn's correction for multiple comparisons; (C) Two-way ANOVA with Tukey's correction for multiple comparisons; **p< 0.01, ****p< 0.0001.

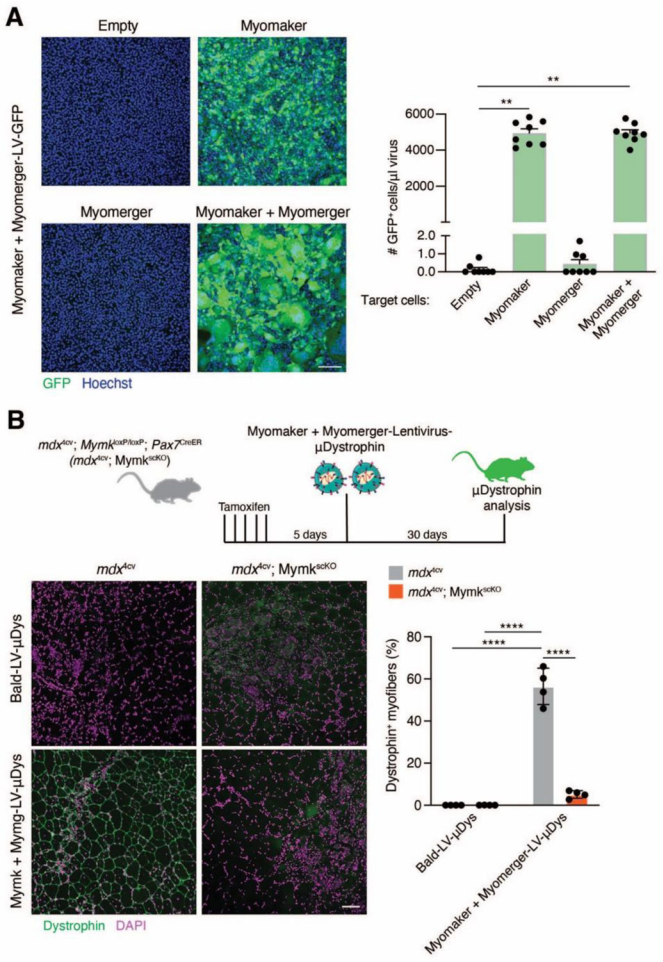

Figure 4. Myomaker is needed on target cells for transduction by Myomaker+Myomerger lentiviruses.

(A) Lentiviruses pseudotyped with Myomaker and Myomerger were placed on BHK21 target cells expressing one or both fusogens. Representative images for GFP^+ cells are shown. Scale bar, 100 µm. Quantification of GFP^+ cells, as a metric for viral transduction, is shown to the right.

(B) *Mdx*^{4cv}; *Mymk*$^{loxP/loxP}$; *Pax7*^{CreER} mice were used to delete Myomaker in myogenic progenitors. Top panel shows schematic for Myomaker deletion and intramuscular delivery of Bald-LV-µDys or Mymk+Mymg-LV-µDys. Bottom left panel shows representative images of sections immunostained with dystrophin antibodies. Nuclei were stained with DAPI. Scale bar, 100 µm. Bottom right panel shows quantification of $µDys^+$ myofibers.

Data are presented as mean ± standard deviation. Statistical tests used were (A) One-way ANOVA (Kruskal-Wallis test) with Dunn's correction for multiple comparisons; (B) Two-way ANOVA with Tukey's correction for multiple comparisons; **p<0.01, ****p<0.0001.

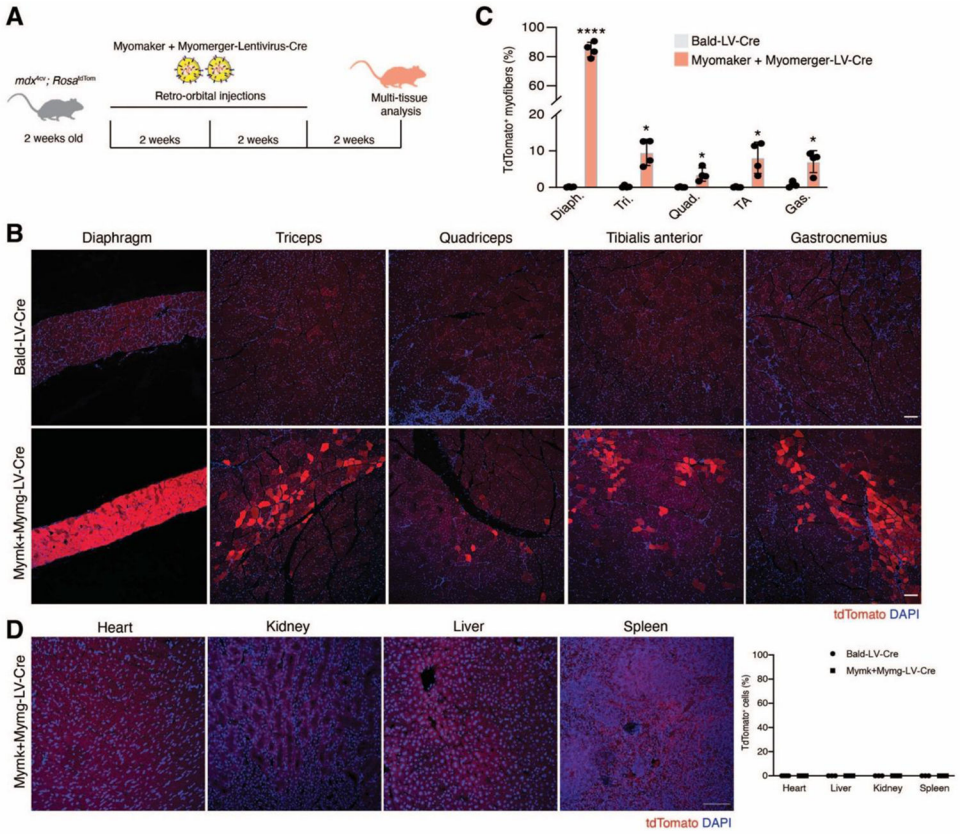

Figure 5. Tropism of Myomaker+Myomerger lentiviruses is specific for skeletal muscle after systemic delivery.

(A) Schematic of experimental plan to assess transduction of lentiviruses delivered to *mdx*^{4cv}; *Rosa*^{tdTom} mice through three retro-orbital injections two weeks apart.

(B) Representative images showing tdTomato^{+} myofibers from various skeletal muscle tissues after retro-orbital delivery of Cre-encoding lentiviruses pseudotyped with Bald or Myomaker and Myomerger. Nuclei were stained with DAPI. Scale bar, 100 μm.

(C) Quantification of the percentage of tdTomato^{+} myofibers.

(D) Representative images analyzing tdTomato^{+} cells from non-skeletal muscle tissues. No positive cells were detected. Quantification is shown on the right. Nuclei were stained with DAPI. Scale bar, 100 μm.

Data are presented as mean ± standard deviation and combined from at least two independent lentiviral preparations. Statistical tests used were (C) Unpaired t-tests with Welch's correction; *p<0.05, ****p<0.0001.

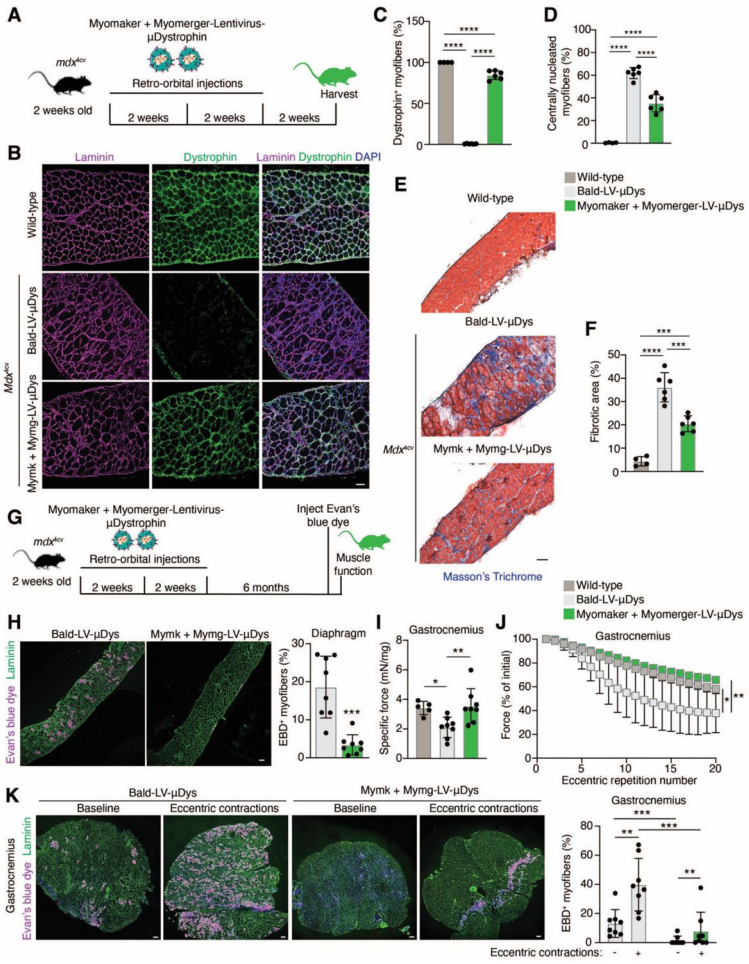

Figure 6. Lentiviruses pseudotyped with the muscle fusogens deliver therapeutic material to skeletal muscle.

(A) Design to assess systemic delivery of Mymk+Mymg-LV-µDys to *mdx*^{4cv} mice.

(B) Immunostaining for dystrophin in *mdx*^{4cv} diaphragms treated with Bald-LV-µDys or Mymk+Mymg-LV-µDys. Nuclei were stained with DAPI. Scale bar, 50 µm.

(C) Quantification of µDys^{+} myofibers in diaphragms.

(D) Quantification of centrally nucleated myofibers in the diaphragms from wild-type mice and mice treated with Bald-LV-µDys or Mymk+Mymg-LV-µDys.

(E) Masson's trichrome staining of diaphragms treated systemically with the indicated lentiviruses. Scale bar, 100 µm.

(F) Quantification of blue trichrome area from (E).

(G) Schematic for long-term assessment of dystrophic muscle after treatment with Mymk+Mymg-LV-µDys.

(H) Representative images from diaphragms showing Evan's blue dye (EBD) myofibers. Scale bar, 100 µm. Quantification is shown on the right.

(I) Specific force from wild-type gastrocnemius muscles, or *mdx*^{4cv} gastrocnemius muscles after systemic treatment with Bald-LV-µDys or Mymk+Mymg-LV-µDys.

(J) Loss of force from gastrocnemius muscles from the indicated mice after eccentric contractions.

(K) Analysis of EBD in gastrocnemius muscles at baseline or after eccentric contractions in *mdx*^{4cv} mice treated with Bald-LV-μDys or Mymk+Mymg-LV-μDys. Scale bar, 200 μm. Quantification is shown on the right.

Data are presented as mean ± standard deviation and combined from at least two lentiviral preparations. Statistical tests used were (C,D,F, I) One-way ANOVA with Tukey's correction for multiple comparisons; (H) Mann-Whitney test; (J) Repeated measures two-way ANOVA with Geisser-Greenhouse correction and Holm-Sidak's corrections for multiple comparisons; (K) Two-way ANOVA with Tukey's correction for multiple comparisons; *p<0.05, **p<0.01, ***p<0.001, ****p<0.0001.

KEY RESOURCES TABLE

REAGENT or RESOURCE	SOURCE	IDENTIFIER
Antibodies		
Rabbit anti-Myomaker	Dr. Leonid Chernomordik laboratory	N/A
Sheep anti- Myomerger	R&D	Cat #AF4580
Mouse anti-VSV-G	Kerafast	Cat #8G5F11
Mouse anti-V5	Invitrogen	Cat #R96025
Mouse anti-VSV-M	Kerafast	Cat #23H12
Mouse anti-VSV-N	Kerafast	Cat #10G4
Rabbit anti-HIV-Gag (p55, p24, p17)	Abcam	Cat #ab63917
Mouse anti-GAPDH	Millipore	Cat #MAB374
Mouse anti-Dystrophin	DSHB	Cat #MANEX1011B (1C7)
Goat anti-Myomaker	Santa Cruz	Cat #SC-244459
Mouse anti-Dystrophin (Dy10/12B2)	GeneTex	Cat # GTX01869
Rabbit anti-Laminin	Sigma Aldrich	Cat #L9393
Mouse anti-Integrin α7	MBL International	Cat # K0046-3
CD45 Monoclonal Antibody (30-F11), Alexa Fluor™ 700	eBioscience	Cat #56-0451-80
CD31 (PECAM-1) Monoclonal Antibody (390), PerCP-eFluor™ 710	eBioscience	Cat #46-0311-80
Ly-6A/E (Sca-1) Monoclonal Antibody (D7), Alexa Fluor™ 700	eBioscience	Cat #56-5981-80
TER-119 Monoclonal Antibody (TER-119), Alexa Fluor™ 700	eBioscience	Cat #56-5921-80
Goat anti-rabbit IgG (H+L) (DyLight™ 680 Conjugate)	Cell Signaling Technology	Cat #5366
Goat anti-Rabbit IgG (H+L) (DyLight™ 800 4X PEG Conjugate)	Cell Signaling Technology	Cat #5151
Donkey anti-Sheep IgG (H+L) Cross-Adsorbed Secondary Antibody, Alexa Fluor™ 680	Invitrogen	Cat #A-21102
Goat anti-mouse IgG (H+L) (DyLight™ 680 Conjugate)	Cell Signaling Technology	Cat #5470
Goat anti-mouse IgG (H+L) (DyLight™ 800 4X PEG Conjugate)	Cell Signaling Technology	Cat #5257
Donkey anti-Mouse IgG Secondary Antibody, IRDye® 680RD	LI-COR	Cat #926-68072
Donkey anti-Goat IgG (H+L) (EM Grade), 12 nm Colloidal Gold AffiniPure	Jackson ImmunoResearch	Cat #705-205-147
Donkey anti-Sheep IgG (H+L) (EM Grade), 6nm Colloidal Gold AffiniPure	Jackson ImmunoResearch	Cat #713-195-147
Donkey anti-Mouse IgG (H+L) (EM Grade), 12 nm Colloidal Gold AffiniPure	Jackson ImmunoResearch	Cat #715-205-150
Goat anti-Mouse IgG (H+L) Cross-Adsorbed Secondary Antibody, Alexa Fluor™ 488	Invitrogen	Cat #A-11001
F(ab')2-Goat anti-Mouse IgG (H+L) Cross-Adsorbed Secondary Antibody, Alexa Fluor™ 546	Invitrogen	Cat #A-11018
Goat anti-Mouse IgG2a Cross-Adsorbed Secondary Antibody, Alexa Fluor™ 568	Invitrogen	Cat #A-21134
Goat anti-Mouse IgG2a Cross-Adsorbed Secondary Antibody, Alexa Fluor™ 488	Invitrogen	Cat #A-21131
Donkey anti-Rabbit IgG (H+L) Highly Cross-Adsorbed Secondary Antibody, Alexa Fluor™ 555	Invitrogen	Cat #A-31572

REAGENT or RESOURCE	SOURCE	IDENTIFIER
Donkey anti-Rabbit IgG (H+L) Highly Cross-Adsorbed Secondary Antibody, Alexa Fluor™ 488	Invitrogen	Cat #A-21206
Bacterial and virus strains		
Stellar Competent Cells	Takara Bio	Cat #636763
Ready-to-use AAV9 Virus (100 µL at titer ≥ 1×1013 vg/mL	Addgene	Cat #105537-AAV9
Chemicals, peptides, and recombinant proteins		
Hy-Clone DMEM high glucose	Cytiva	Cat #SH30022.01
Gibco DMEM, High Glucose	Gibco	Cat #11965118
Ham's F10, with L-Glutamine	Cytiva	Cat #SH30025.01
Ham's F-10 nutrient mixture	Gibco	Cat #11550043
USDA Origin FBS	Peak Serum	Cat #PS-FB2
FBS - USDA Origin Pure Premium, Tet-Free	Peak Serum	Cat # PS-FB3
Horse Serum, heat inactivated, New Zealand origin	Gibco	Cat # 26050088
Sodium Pyruvate (100 mM)	Gibco	Cat #11360070
Penicillin-Streptomycin (5,000 U/mL)	Gibco	Cat #15070063
L Glutamine (200mM)	Gibco	Cat #25030081
Doxycycline Hydrochloride, Ready Made Solution	Sigma Aldrich	Cat # D3072
Recombinant Human FGF-basic	PeproTech	Cat #100-18C
Matrigel® Basement Membrane Matrix	Corning	Cat #354234
Puromycin Dihydrochloride	Gibco	Cat #A1113802
Blasticidin S HCl	Gibco	Cat #A1113903
FuGENE-6	Promega	Cat #E2692
Polyethylenimine (PEI)	Polysciences	Cat #24314-2
Collagenase, Type 2	Worthington Biochemical	Cat # LS004176
Pronase, from Streptomyces griseus	Sigma Aldrich	Cat #10165921001
HEPES (1 M)	Gibco	Cat #15630106
Vybrant® Multicolor Cell-Labeling Kit (DiO, DiI, DiD Solutions, 1 mL each)	Invitrogen	Cat #V22889
DPBS without Calcium and Magnesium	Gibco	Cat #14190250
Ultrapure DNase RNase free water	Invitrogen	Cat #10977023
Acetone	Sigma Aldrich	Cat # 320110
Paraformaldehyde, 16% w/v aq. soln., methanol free	Thermo Scientific	Cat # 43368
Cardiotoxin	EMD Millipore	Cat #217503-1MG
Evans blue dye	Sigma Aldrich	Cat #E2129-10G
D-luciferin	Promega	Cat #E1605
D-luciferin	Goldbio	Cat #LUCK-2G
Hoechst 33342	Invitrogen	Cat #H3570
Vectashield Antifade Mounting Medium with DAPI	Vector Laboratories	Cat #H1200
Ammonium molybdate tetrahydrate	Sigma Aldrich	Cat #A7302-100G
Phosphotungstic Acid (PTA)	Electron Microscopy Sciences	Cat #19500
Masson Trichrome Kit	Richard-Allan Scientific	Cat # 22-110-648

REAGENT or RESOURCE	SOURCE	IDENTIFIER
Halt™ Protease Inhibitor Cocktail, EDTA-Free (100X)	Thermo Scientific	Cat #78437
Phosphatase Inhibitor Cocktail 2	Sigma Aldrich	Cat #P5726
Bio-Rad Protein Assay Dye Reagent Concentrate	BioRad	Cat #5000006
Critical commercial assays		
InFusion HD cloning plus Kit	Clonetech	Cat #638909
Experimental models: Cell lines		
Mouse primary myoblasts from C57BL/6J mice	This study	N/A
C2C12 cells	ATCC	Cat #CRL-1772
C3H/10T1/2 fibroblasts	ATCC	Cat #CCL-226
BHK21 cells	Kaariainen et al.[54]	N/A
293T/17 (HEK 293T/17)	ATCC	Cat #CRL-11268
Platinum-E retroviral packaging cells	Cell Biolabs	Cat #RV-101
Dox-inducible Empty-BHK21 cells	This study	N/A
Dox-inducible-EFF1-V5 BHK21 cells	This study	N/A
Dox-inducible-Myomaker BHK21 cells	This study	N/A
Dox-inducible-Myomerger BHK21 cells	This study	N/A
Dox-inducible-Myomaker+Myomerger BHK21 cells	This study	N/A
Dox-inducible-Empty-Cre-reporter BHK21 cells	This study	N/A
Dox-inducible-Myomaker+Myomerger-Cre-reporter BHK21 cells	This study	N/A
Dox-inducible Empty-HEK293t cells	This study	N/A
Dox-inducible Myomaker-HEK293t cells	This study	N/A
Dox-inducible Myomerger-HEK293t cells	This study	N/A
Dox-inducible Myomaker+Myomerger-HEK293t cells	This study	N/A
Experimental models: Organisms/strains		
Mouse: C57BL/6J	The Jackson Laboratory	Cat #000664
Mouse: *Mdx*^{4cv} (B6Ros.Cg-Dmdmdx-4Cv/J)	The Jackson Laboratory	Cat #002378
Mouse: *Rosa26*^{tdTomato} (B6;129S6-Gt(ROSA)26Sortm9(CAG-tdTomato)Hze/J)	The Jackson Laboratory	Cat #007905
Mouse: *Mdx*^{4cv}; *Rosa26*^{tdTomato}	Mitani et al.[55]	N/A
Mouse: *Mdx*^{4cv}; *Mymk*$^{loxP/loxP}$; *Pax7*^{CreER}	Petrany et al.[37]	N/A
Recombinant DNA		
pLVX-TetOne-Puro	Clontech	Cat #631849
pLVX-TetOne-Blast	This study	Modified from Cat #631849
pLVX-TetOne-EFF1-V5-Puro	This study	N/A
pLVX-TetOne-Myomaker-Puro	This study	N/A
pLVX-TetOne-Myomerger-Puro	Leikina et al.[15]	N/A
pLVX-TetOne-Myomerger-Blast	This study	N/A
pLVX-TetOne-EFF1-V5-Puro	This study	N/A
pMD2.G	Addgene	Cat #12259

REAGENT or RESOURCE	SOURCE	IDENTIFIER
psPAX2	Addgene	Cat #12260
Cre reporter	Addgene	Cat #62732
pLX304-Luciferase-V5	Addgene	Cat #98580
pLX304-GFP	Yang et al.[56]	N/A
pLKO.1-puro-eGFP	Sigma Aldrich	Cat #SHC005
pLKO.1-puro-Cre	This study	N/A
pLX304-μDys5	This study	N/A
pBabeX-Empty	Millay et al.[10]	N/A
pBabeX-Myomaker	Millay et al.[10]	N/A
pBabeX-Myomerger	Quinn et al.[11]	N/A
Software and algorithms		
Fiji	ImageJ	https://fiji.sc
Living Image 4.7.3 software	PerkinElmer	https://www.perkinelmer.com/lab-products-and-services/resources/in-vivo-imaging-software-downloads.html#LivingImage
FlowJo v10.8.1	FlowJo	https://www.flowjo.com/solutions/flowjo
Graphpad Prism v9	Graphpad Prism Inc	https://www.graphpad.com/scientific-software/prism/
Adobe Illustrator	Adobe	https://www.adobe.com/products/illustrator.html
Other		
Cytation™ 5	BioTek	https://www.biotek.com/products/imaging-microscopy-cell-imaging-multi-mode-readers/cytation-5-cell-imaging-multi-mode-reader/
Countess 3 FL Automated Cell Counter	Invitrogen	https://www.thermofisher.com/order/catalog/product/AMQAF2000
Odyssey infrared detection system	LI-COR Biosciences	https://www.licor.com/bio/support/answer-portal/imaging-systems/odyssey-clx.html
H-7650 Transmission Electron Microscope	Hitachi	https://www.hitachi-hightech.com/us/
Nikon Eclipse Ti inverted microscope	Nikon	https://www.microscope.healthcare.nikon.com/products/inverted-microscopes/eclipse-ti-series
Nikon Eclipse Ti inverted microscope with A1R confocal running NIS Elements	Nikon	https://www.microscope.healthcare.nikon.com/products/confocal-microscopes/a1hd25-a1rhd25

REAGENT or RESOURCE	SOURCE	IDENTIFIER
300C-LRmuscle lever system	Aurora Scientific Inc	https://aurorascientific.com/products/muscle-physiology/controllers-levers-transducers/300c-dual-mode-muscle-levers/
IVIS spectrum CT in vivo imaging system	PerkinElmer	Cat #128201
FACSCanto	BD Biosciences	https://www.bdbiosciences.com/en-us/products/instruments/flow-cytometers/clinical-cell-analyzers/facscanto
LSRFortessa	BD Biosciences	https://www.bdbiosciences.com/en-us/products/instruments/flow-cytometers/research-cell-analyzers/bd-lsrfortessa